



Cite this: *Soft Matter*, 2022,  
18, 7464

## Multicomponent and multifunctional integrated miniature soft robots

Neng Xia,<sup>a</sup> Guangda Zhu,<sup>a</sup> Xin Wang,<sup>a</sup> Yue Dong<sup>a</sup> and Li Zhang  <sup>abcd</sup>

Miniature soft robots with elaborate structures and programmable physical properties could conduct micromanipulation with high precision as well as access confined and tortuous spaces, which promise benefits in medical tasks and environmental monitoring. To improve the functionalities and adaptability of miniature soft robots, a variety of integrated design and fabrication strategies have been proposed for the development of miniaturized soft robotic systems integrated with multicomponents and multifunctionalities. Combining the latest advancement in fabrication technologies, intelligent materials and active control methods enable these integrated robotic systems to adapt to increasingly complex application scenarios including precision medicine, intelligent electronics, and environmental and proprioceptive sensing. Herein, this review delivers an overview of various integration strategies applicable for miniature soft robotic systems, including semiconductor and microelectronic techniques, modular assembly based on self-healing and welding, modular assembly based on bonding agents, laser machining techniques, template assisted methods with modular material design, and 3D printing techniques. Emerging applications of the integrated miniature soft robots and perspectives for the future design of small-scale intelligent robots are discussed.

Received 1st July 2022,  
Accepted 10th September 2022

DOI: 10.1039/d2sm00891b

[rsc.li/soft-matter-journal](http://rsc.li/soft-matter-journal)

### 1. Introduction

Small-scale soft robots are a class of controllable devices with inherent compliance and maximum sizes in millimeters that

can actively interact with the environment.<sup>1–9</sup> Miniature soft robots have attracted extensive research interest due to their promising applications in minimally invasive therapies, precision medicine, environmental monitoring systems, and biomimetic locomotion. Due to their large deformability and miniaturized structure, these machines can move flexibly through unstructured and narrow terrains (e.g., eustachian tube models, small intestinal tissue, and brachial artery). The highly controllable structural deformation of the miniature robots enables them to imitate the locomotion of living organisms such as cilia arrays, starfish larvae, midge larvae, and

<sup>a</sup> Department of Mechanical and Automation Engineering, The Chinese University of Hong Kong, Hong Kong, China. E-mail: [lizhang@cuhk.edu.hk](mailto:lizhang@cuhk.edu.hk)

<sup>b</sup> Chow Yuk Ho Technology Center for Innovative Medicine, The Chinese University of Hong Kong, Hong Kong, China

<sup>c</sup> CUHK T Stone Robotics Institute, The Chinese University of Hong Kong, Hong Kong, China

<sup>d</sup> Department of Surgery, The Chinese University of Hong Kong, Hong Kong, China



Neng Xia

Neng Xia received a B.Eng degree from Central South University, Changsha, China, in 2016, and an MS degree from Zhejiang University, Hangzhou, China, in 2019, both in mechanical engineering. He is currently working toward the PhD degree with The Chinese University of Hong Kong, Hong Kong, China. His research interests include magnetic soft robots, hydrogel materials, and 3-D printing.



Guangda Zhu

Guangda Zhu is currently a Postdoctoral Fellow in the Department of Mechanical and Automation Engineering at The Chinese University of Hong Kong. He received his PhD degree at the Institute of Chemistry, Chinese Academy of Sciences (2021). His research interests include new materials for 3D printing, dynamic polymers, functional polymer composites and soft robotics.

jellyfish and provides robotic platforms to unveil their underlying physical mechanisms.<sup>10–14</sup> In addition, the development of smart materials (such as stimuli-responsive materials, self-healing materials, and biomaterials) and fabrication technologies endow miniature soft robots with various functionalities, further promoting their practical applications.<sup>15–18</sup>

To imitate the versatility and adaptability of natural organisms, miniature soft robotic systems with heterogeneous architectures need to be constructed. A robotic system with a single material composition, such as a robot body with an actuation unit, could perform specific tasks based on its shape-morphing or locomotion properties, *e.g.*, manipulating objects.<sup>19–28</sup> However, with the increasing complexity of application scenarios, it is necessary to integrate multiple functional modules with different material compositions in the soft robotic system.<sup>29–32</sup> For example, when wireless micro-robots are used for monitoring complex environments, it is necessary to load units with sensing, communication, and energy supply functions on the robot body. When performing precision medical

functions, microrobots need to integrate therapeutic modules such as cells or drugs to reach designated locations.<sup>2,3,26,33–37</sup> In addition, in order to develop a small-scale robotic system with high reliability, it is necessary to load a positioning and navigation module and a somatosensory unit on the robot body to monitor the deformation of the robot. The seamless integration of robotic structures and various functional modules remains a key scientific challenge.

An intelligent integration method could ensure the cooperative operation of multiple units in the miniature robotic system and the high reconfigurability of the system to adapt to an unstructured environment.<sup>38</sup> Various technologies have been proposed to achieve the seamless integration of multiple components, including semiconductor and microelectronic techniques, modular assembly based on self-healing and welding, modular assembly based on bonding agents, laser machining technique, template assisted method with modular material design, and 3D printing techniques.<sup>10,39–45</sup> This review intends to provide an overview of the latest development in multi-component and multifunctional integrated miniature soft robots and a perspective for future multifunctional miniature robots. The diverse actuation units and functional units for soft robotic systems are introduced at the beginning and the available integration methods are summarized (Fig. 1). The emerging applications and functions of integrated miniature soft robots are highlighted, including biomedical applications, environmental and proprioceptive sensing, and intelligent electronics. Finally, the conclusions and outlooks toward intelligent miniature robotic systems are discussed.



**Xin Wang**

*Xin Wang is a PhD student in the Department of Mechanical and Automation Engineering, The Chinese University of Hong Kong, Hong Kong, SAR 999077. His research interests include soft actuators and robotics, hydrogel-based devices and light driven micro/nano robots.*



**Yue Dong**

*Yue Dong received his PhD degree in 2019 from the College of Life Science and Technology, Huazhong University of Science and Technology, China. Currently, he is working as a postdoctoral fellow in the Department of Mechanical and Automation Engineering, The Chinese University of Hong Kong, Hong Kong, SAR 999077. His research interests include programmable actuators, soft magnetic robots, robot swarm, graphene assembly, and microfluidics.*

## 2. Multiple units for miniature soft robots

Robots discussed in this review are defined as machines consisting of sensing units, actuation devices, control units, and



**Li Zhang**

*Li Zhang is a professor in the Department of Mechanical and Automation Engineering and a professor by courtesy in the Department of Surgery at The Chinese University of Hong Kong (CUHK). He is also a director of the SIAT-CUHK Joint Laboratory of Robotics and Intelligent Systems. Before he joined CUHK as an assistant professor in 2012, he worked in Prof. Bradley Nelson's group as a postdoc and then as a senior scientist and lecturer in the Institute of Robotics and Intelligent Systems, ETH Zurich, Switzerland. Dr Zhang's main research interests include small-scale robotics and their applications for translational biomedicine. He is a Fellow of the Royal Society of Chemistry (FRSC).*

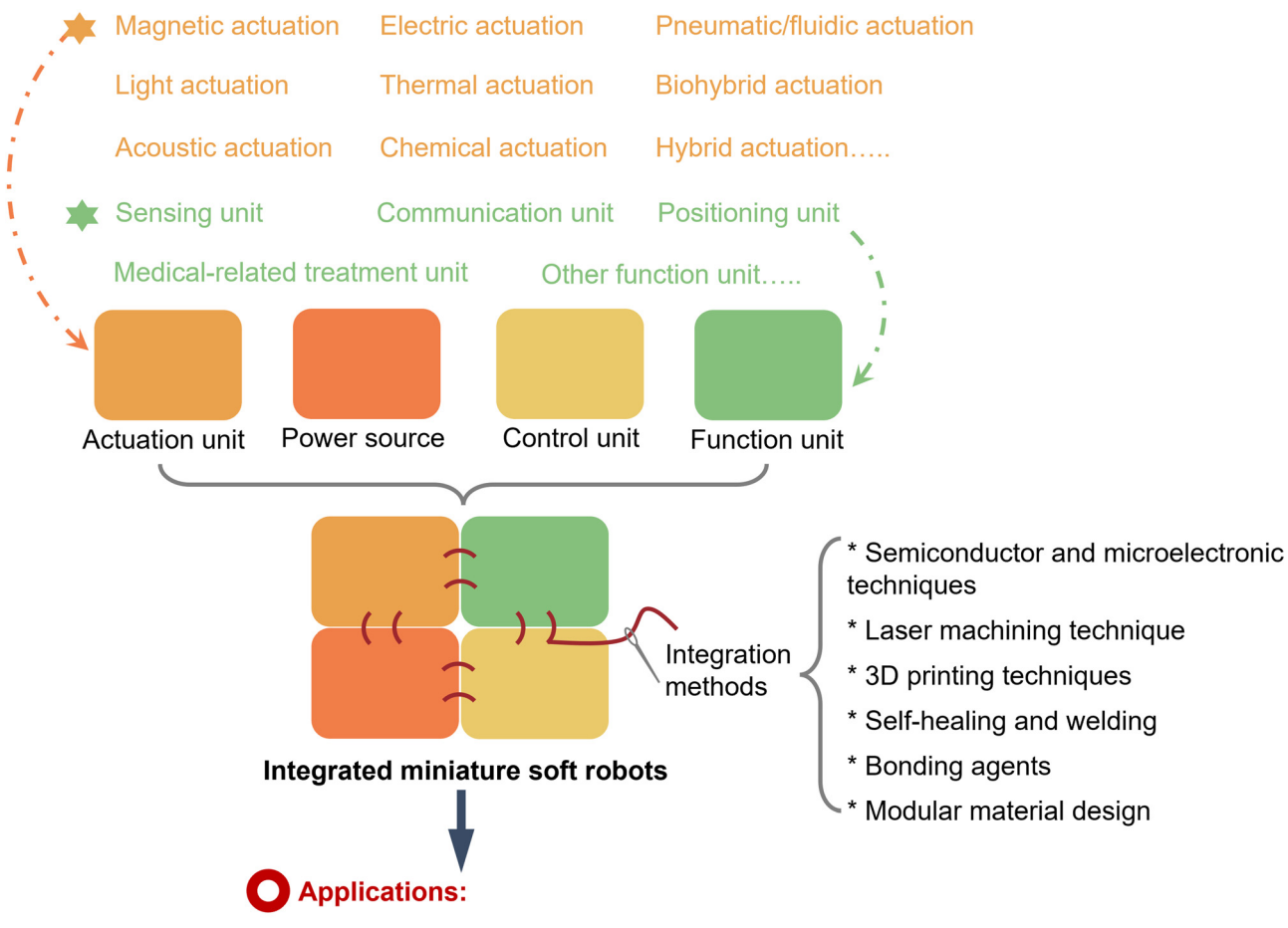


Fig. 1 Schematic illustration of multicomponent and multifunctional integrated miniature soft robots, including representative actuation units, functional units, and emerging applications.

energy supplies, and are capable of completing the required deformation or locomotion as well as performing specified tasks.<sup>9,46,47</sup> In comparison, actuators refer to highly deformable materials that can generate desired motions, output force, or torque under external stimuli.<sup>48</sup> Robotic systems require a high integration of actuation and sensing mechanisms with the robot body, which poses challenges for the fabrication of small-scale robots due to their limited on-board space. Therefore, we mainly discuss the integration methods of small-scale robotic systems and their multifunctional applications. Heterogeneous architectures that combine multi-material components or multiple functional units into an integrated system are important for creating multifunctional and physically adaptable miniaturized soft robots. It has become a hotspot research topic to develop strategies that could load the actuation unit and various functional units with high integration density on the robot body constructed of engineering materials and to ensure the cooperative work of each unit. Herein, we

discuss actuation units and common functional units used for the integrated robotic system and Table 1 summarizes the engineering materials applied for the robotic body.

## 2.1 Actuation power for miniature soft robots

**2.1.1 Magnetic actuation.** Magnetic small-scale robots can be driven by magnetic torques or magnetic field forces based on magnetic field gradients.<sup>49–51</sup> Due to the good programmability of the magnetic actuation methods, researchers have developed a variety of biomimetic locomotion modes, such as those of jellyfish, zebrafish larvae, midge larvae, scallops, and multilegged animals.<sup>12–14,52,53</sup> The programmability of the magnetic actuation method derives from the design of the magnetic field and the distribution of magnetic domains inside the robot. Soft robots with heterogeneous 3D magnetization profiles can exhibit complex 2D-to-3D and 3D-to-3D structural changes, including complex surface with diverse Gaussian curvature.<sup>7,54</sup> A variety of fabrication techniques have been

Table 1 Comparison of engineering materials for robot body and compatible integration methods

Materials	Young's modulus (MPa)	Integration methods	Application
Shape memory polymers	2–1200	Semiconductor and microelectronic techniques, self-healing and welding	Environmental measurements, modular morphing devices <sup>2,41</sup>
Hydrogel + polyimide	—	Semiconductor and microelectronic techniques	Minimally invasive surgery, wireless power transfer <sup>72,109</sup>
Platinum	150 000–180 000	Semiconductor and microelectronic techniques	Silicon-based, functional robots, artificial cilia <sup>10,39</sup>
Magnetic dynamic polymer	0.4–1.2	Self-healing and welding	Reconfigurable morphing devices <sup>40,122</sup>
Liquid crystal elastomer	0.5–37.6	Self-healing and welding, Modules bonding with bonding agents	Multifunctional soft robots <sup>42,69,123,126</sup>
Polydimethylsiloxane	1.2–4.2	Modules bonding with bonding agents, surface modification	Soft capsules, peristaltic pump, and anchoring machine, functional circuits, environmental sensing <sup>43,57,133</sup>
Silicon elastomer	0.01–0.1	Modules bonding with bonding agents, 3D printing	Soft capsules, peristaltic pump, and anchoring machine, environmental inspection, minimally invasive surgery <sup>45,57,127,156</sup>
Adhesive sticker	0.1 (shear modulus)	Modules bonding with bonding agents	Precision medicine, environmental sensing, circuit repairing <sup>37</sup>
Hydrogel + silicone elastomer	0.007–5	3D printing	Cardiovascular stent, pneumatic actuator <sup>154</sup>
SU-8	4800	3D printing	Artificial musculoskeletal systems <sup>155</sup>

developed to form heterogeneous magnetization distribution of soft robots, including 3D printing, photolithography, template-assisted magnetic programming, laser heating, and modular assembly based on dynamic covalent bonds or bonding agents.<sup>7,26–28,40,55–58</sup> The integration of advanced fabrication techniques and magnetization programming strategies greatly enhances the functionalities and application potential of magnetic miniature robots.

**2.1.2 Light actuation.** The high spatial resolution of the light-driven approaches enables precise and selective control. For example, Li *et al.* proposed a single material component of liquid crystal elastomer (LCE) based cilia, which can generate a series of complex motion behaviors such as twisting, bending, phototropic, and photophobic motions *via* a tunable light source.<sup>59</sup> Currently, a variety of light-responsive materials have been developed for the construction of soft robots, such as LCE, supramolecular hydrogels, graphene oxide, and composites based on photothermal conversion.<sup>23,30,60</sup>

**2.1.3 Acoustic actuation.** Due to their good adaptability and deep tissue penetration ability, acoustic waves have a wide range of applications in the biomedical field. Many microrobots based on acoustic radiation force or bubble assistance have been developed.<sup>20,61</sup> They could rotate, slide, and achieve pull-type motions on the surface of objects, move along vertical walls, and imitate starfish larvae-like motions.<sup>11,61,62</sup> To develop acoustic actuation in a selective and accurate manner, precise acoustic field control strategies such as phased array acoustic waves, acoustic holography methods, and time-lapse Fourier synthetic harmonics have been proposed.<sup>63,64</sup>

**2.1.4 Electric actuation.** The electric actuation method has a fast response capability and is widely used to actuate soft robots based on polyelectrolyte hydrogels, dielectric elastomers, and metal films.<sup>65,66</sup> It has been demonstrated that this actuation method can be integrated with complementary metal-oxide-semiconductor (CMOS) clock circuits and shows

good programmable features.<sup>10</sup> Using electric field control, it enables fast transition behavior with a bistable mechanism, human-like walking motion, cilia-inspired non-reciprocal motions, and reversible large out-of-plane deformation.<sup>10,65–67</sup> They have broad application prospects including fluid manipulation, optical zoom system, optical switch, and pulse pumps.<sup>10,65,66</sup>

**2.1.5 Thermal actuation.** The direct transfer of heat to robots at the small-scale size is relatively difficult. Photothermal conversion, electrical heating, and electromagnetic heating are often adopted to build temperature-responsive robots, such as poly(*N*-isopropylacrylamide) (pNIPAM) hydrogel, shape memory polymer (SMP), and LCE based robots.<sup>44,68,69</sup> In addition, Wang *et al.* and Dong *et al.* applied the temperature gradient generated by the hot plates to actuate soft robots with self-oscillating behaviors.<sup>30,70</sup> Through structural design, the robots were able to achieve continuous rolling, rotation, and crawling locomotion on hot plates.

**2.1.6 Chemical actuation.** Chemical actuation involves the use of bubbles generated by chemical reactions or chemical gradients to propel miniature robots.<sup>71</sup> Chemical actuation can provide high swimming velocities in the presence of abundant chemical fuels, but the continuous supply of chemical fuel is relatively difficult in real environments and the fuels are often toxic.<sup>72</sup> In addition, self-oscillating chemical reactions, such as the Belousov–Zhabotinsky reaction, have also been used to construct soft robots with a self-propelled behavior, but the controllability and swimming speeds of soft robots based on self-oscillating chemical reactions still need to be improved.<sup>73</sup>

**2.1.7 Pneumatic/fluidic actuation.** Pneumatic or fluidic actuation has a wide range of applications in soft robots. Through the design of the channels, they can achieve bending, twisting, and complex three-dimensional deformations, such as the shape of a human face under the action of the drive source.<sup>74,75</sup> Based on pneumatic or fluid drives, robotic

prototypes such as artificial muscles, grippers, and multi-legged robots have been developed.

**2.1.8 Biohybrid actuation.** Biohybrid actuation refers to soft robotic systems constructed by integrating living organisms and flexible materials. They have the advantages of high output force and high power density in small-scale robotic actuation.<sup>76</sup> Cardiomyocytes, skeletal muscle cells, microorganisms, sperm, *etc.* are used as power sources for biohybrid soft robots.<sup>76,77</sup> Utilizing the stimuli-responsive behaviors of biological components, highly controllable biohybrid soft robotic systems have been developed, which have practical application prospects in the fields of drug delivery, organ-on-a-chip, tissue engineering, cell manipulation, and minimally invasive surgery.<sup>78,79</sup> Natural organisms provide a wealth of inspiration for the design and actuation of robots, enabling robotic systems to achieve intelligence close to that of their counterparts. Katzschmann *et al.* developed a hydraulically driven robotic fish system that can navigate in the depth range of 0–18 m.<sup>80</sup> Under external commands, the robotic fish can observe marine life and explore the surrounding environment. Yoerger *et al.* proposed marine robots capable of tracking the movements of jellyfish and larvae at depths of 200 m.<sup>81</sup> Inspired by marine vertebrates, Lee *et al.* developed a flatfish-like robot that can be controlled by soft thermoelectric pneumatic actuators and can move freely in three dimensions in the water.<sup>82</sup> Small-scale biohybrid robots have been proven to be able to complete locomotion modes such as crawling, rolling, and swimming, but scaling up the biohybrid robots, such as mass fabrication of biohybrid robots beyond the centimeter level, remains challenging.<sup>83</sup> Further research in terms of tissue survival, the interaction of biological interfaces and the control methods of biological tissues are still needed.

**2.1.9 Hybrid actuation.** A single actuation mode would exhibit limitations when dealing with complex real environments, such as the lack of precise directional control for acoustic actuated robots, the limited penetration depth of light actuation, and the attenuation of magnetic field strength over distance. Hybrid actuation mechanisms could combine key features and advantages of different actuation modes to improve the locomotion performance and controllability of the robots. For instance, the precise directional control capability of magnetic actuation is expected to improve the maneuverability of microrobots based on acoustic actuation, catalytic propulsion, or biohybrid actuation.<sup>18,84</sup> Ren *et al.* proposed an acoustic-magnetic powered semi-capsule-shaped micro-swimmer.<sup>61</sup> The bubbles trapped in the capsule structure resonate and provide a strong propulsion force under the stimulation of ultrasound, which enables the robot to swim at 350 body length/second to advance. The deposited magnetic nickel layer enables the robot to change the direction and speed of locomotion under the action of an external magnetic field. The proposed hybrid actuation enables the robot to move along vertical boundaries or in free space. Although the magnetically driving method has good steerability, it is a challenge to realize the spatial selective actuation. The combination of magnetic and light actuation could greatly improve the reconfigurability,

selective manipulation, and sequential response capability of the robot. Liu *et al.* used the photothermal response properties of magnetic shape memory materials to lock or soften the shape memory materials, and the hybrid stimulation of magnetism and light enabled the reprogrammable morphologies of soft robots.<sup>85</sup> Han *et al.* constructed an omnidirectional walking crab robot using superparamagnetic nanoparticles and graphene materials.<sup>86</sup> The external magnetic field is used to adjust the center of mass of the robot, and the light field selectively drives the specific joints of the robot to realize the multi-degree-of-freedom shape morphing of the robot and stable omnidirectional walking.

## 2.2 Functional units for miniature soft robots

By integrating various functional modules into intrinsically programmable smart materials and structures, many seamlessly integrated soft robots have been developed to achieve a more powerful performance and multifunction.<sup>87–89</sup> Introducing multiple material compositions to fabricate soft robots with diverse heterogeneous mechanical, electrical, optical, and magnetic properties would significantly enhance the capabilities, mobility, and dexterity of robots.<sup>90–93</sup> Soft robots have broad application prospects in minimally invasive surgery, flexible electronics, and industrial monitoring.<sup>94</sup> Based on the complex application scenarios, miniaturized soft robots need to be able to load a variety of functional modules such as energy supply modules, communication modules, positioning modules, perception modules, and medical-related treatment modules.<sup>95,96</sup>

The integration of flexible sensing units and actuation units endows the miniaturized robot with the ability to perceive the surrounding environment during locomotion or deformation. A variety of materials such as liquid metals, optical fibers, conductive composites, and ion gels have been developed for constructing sensing units for multifunctional robots.<sup>44,97–99</sup> Through embedded somatosensory sensors, optoelectronic sensors or changes in the resistance of the robot body, the deformation of robots can be detected, including bending, expansion, stretching, and compression. Meerbeek *et al.* adopted machine learning techniques and embedded optical fibers to accurately predict the robot's deformation type and deformation magnitude, allowing them to achieve multimodal perception and reliably respond to external stimuli.<sup>97</sup> In addition, distributed sensing units exposed to the external environment can monitor various environmental signals, including pH, temperature, pressure, light, and physiological signals. Various environmental sensing particles, inks, quantum dots, metallic materials, and stimuli-responsive gels have been applied to impart environmental perception capabilities to robots. For example, flexible metal strain gauges can sense normal forces with high sensitivity, and thin metal wires can be used as temperature sensors due to their temperature-dependent resistances.<sup>100</sup> High spatial density integration of sensing units can greatly enhance the functional options of robots. In order to build a highly integrated miniaturized system, the multi-layer stacking technology of flexible

electronics and the seamless integration using adhesive materials have been developed.<sup>101</sup>

Due to the limited onboard space, the wireless power supply of miniaturized soft robots remains a great challenge. By utilizing the piezoelectric effect and magnetic actuation, Lu *et al.* integrated a piezoelectric foam composite into a multi-legged magnetic robot that could generate electricity through the deformation of the foam composite during the robot movement.<sup>102</sup> The output voltage can reach 0.45 V, which can be used for the sensor components carried by the robot. However, due to the relative rigidity of the communication module and energy supply module, the flexibility of the developed multilegged miniature robot is limited. Peng *et al.* proposed a slug-inspired soft robot that combines magnetic actuation and triboelectric nanogenerator technology.<sup>103</sup> This soft robot can move on different terrains with a bioinspired gait and a triboelectric nanogenerator integrated into the robot can convert the pedal waves generated during the movement to triboelectricity which could drive external electronic devices.

### 3. Integration methods for multifunctional miniature soft robots

Integrated methods refer to adopting the all-in-one fabrication strategies to combine multiple functional modules or heterogeneous material components on a small-scale robotic system to effectively enhance the functionality and adaptability of the robot. We classify the integration methods according to the fabrication methods, mainly including semiconductor and microelectronic techniques, laser machining techniques, 3D printing techniques, manual assembly or jig-assisted assembly which is further subdivided into assembly based on self-healing materials, assembly using a bonding agent, and a template assisted method with modular material design (Table 1). Semiconductor and microelectronic techniques allow the selective connection of different materials at predefined sites, and exhibit high manufacturing precision and mass fabrication capabilities for multifunctional miniature robots. A laser machining technique provides a fast and customizable method for the preparation of modular robots. High-energy lasers can cut or engrave a variety of soft materials into preferable patterns. In addition, laser-processed micropatterns can endow robotic structures with selective adhesion or absorption capabilities. Combined with transfer printing technology, 2D or 3D heterogeneous robotic structures can be rapidly constructed. 3D and 4D printing techniques provide a powerful platform to form complex 3D robotic structures, and multi-material 3D printing enables miniaturized robots to powerfully integrate multiple functional modules. Bottom-up assembly methods, such as manual or jig-assisted assembly,<sup>41,57</sup> magnetic-assisted assembly,<sup>40</sup> enable the construction of modular robots with arbitrary material compositions as well as 3D geometries on a small scale, where the connection of different modular units can be achieved by the self-healing property of materials or external bonding agents. The design of modular

composite materials allows the direct construction of robotic systems with both sensing and actuation capabilities, which could avoid potential physical mismatch or interfacial delamination.<sup>44,104</sup>

#### 3.1 Semiconductor and microelectronic techniques

Semiconductor processing technology is widely used in the manufacture of flexible electronic devices, and this type of technology provides powerful solutions for the deposition and etching of diverse materials to form 3D structures. The main advantages of semiconductor processing technology are mass production and easy integration with electronic components. In order to realize complex 3D structures, researchers have developed self-rolling and compressive buckling technology.<sup>72,105-108</sup> By controlling the formation of internal stress, robotic structures integrated with electronic components could exhibit hierarchical 3D layouts. For example, Kim *et al.* developed 3D microfliers loaded with electronic components (e.g., silicon nanofilm transistors and near-field communication (NFC) chips), as shown in Fig. 2(a).<sup>2</sup> The SMP films were patterned by metal hard mask and oxygen plasma reactive ion etching, and a multilayer of Ti/Mg/Ti/SiO<sub>2</sub> was deposited thereon. Hydroxyl groups are formed on the surface of the ozone-treated SiO<sub>2</sub> layer, enabling the SMP film to form strong covalent bonding with the pre-strained silicone elastomer substrate at specific locations. A mechanical buckling mechanism based on pre-strain release would induce the geometric transformation of the film structure from 2D to 3D imitating the structure of wind-dispersed seeds. In the process of preparing the 2D SMP precursor, the electronic components encapsulated by the polyimide can be transfer printed on the SMP film to enable the integration of the electronic components. These flying devices can be released in the air at controlled speeds and perform environmental measurements and monitoring through integrated wireless devices. Rivkin *et al.* introduced a medical catheter integrated with microelectronics through self-rolling technology (Fig. 2(b)).<sup>109</sup> With a diameter of only 0.1 mm, the medical catheter could accommodate actuating units (electrically actuated manipulator) and sensing units (magnetic sensors), and perform fluid delivery by taking advantage of the hollow structure. In addition, Bandari *et al.* proposed a flexible motile microsystem with wireless energy transfer functions to control the propulsion of the microsystem and to power the integrated electronic modules in the microsystem (Fig. 2(c)).<sup>72,110</sup> A microrobotic system consisting of multiple layers of polymers is formed on a substrate and the curling effect induced by the etching of a sacrificial layer guides the formation of tubular structures at the edges of the flexible microsystem. A square coil and heating wire integrated in the microrobotic system could wirelessly transfer energy and heat the catalytic engines to control the production of oxygen. The integrated microelectronic system expands the application scenarios of mobile microrobots.

The development of mobile microrobot systems that are compatible with CMOS circuits has great potential, since they provide an enabling technology to perform programmable and

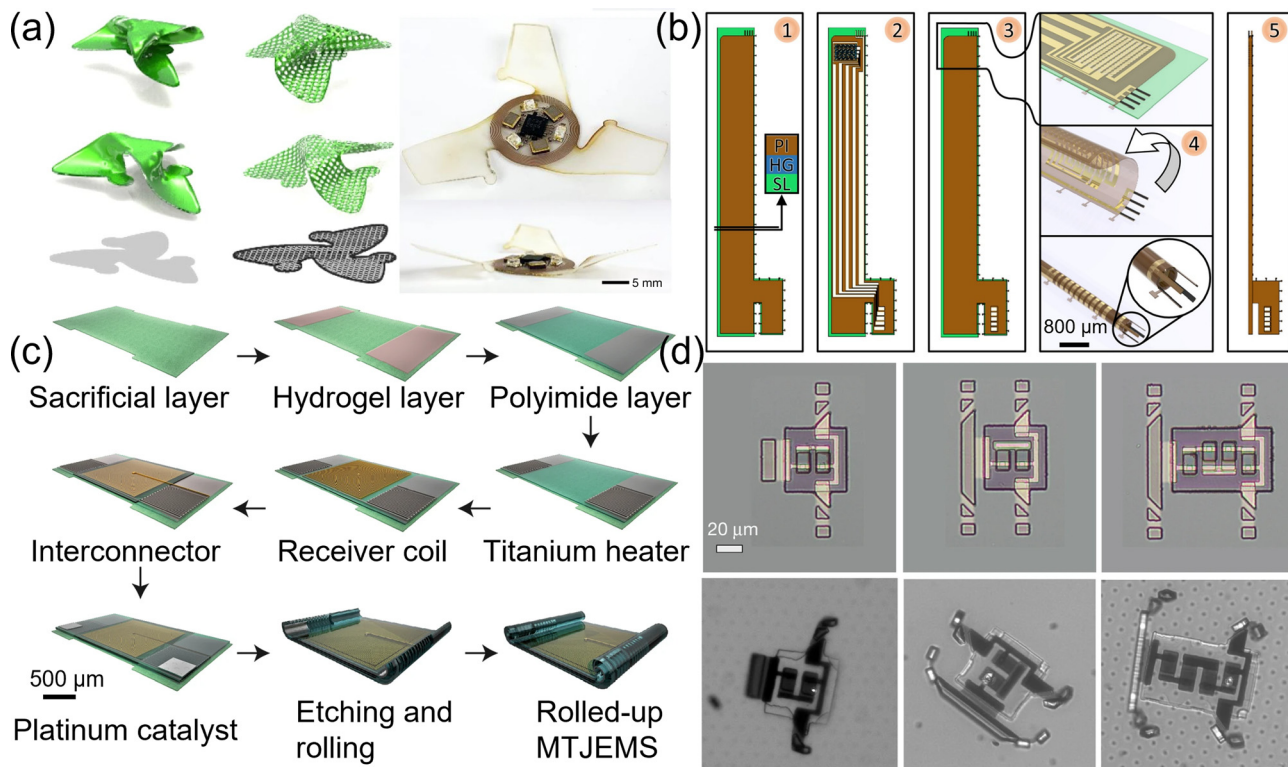


**Fig. 2** Semiconductor and microelectronic techniques. (a) Seed-inspired 3D electronic microflies. Scale bar, 5 mm. Reproduced with permission<sup>2</sup>. Copyright 2021, Spring Nature. (b) Integrated self-assembled catheter with electronic components. Reproduced with permission.<sup>109</sup> Scale bar, 800 μm. Copyright 2021, American Association for the Advancement of Science. (c) Fabrication schematics of a motile twin-jet-engine microsystem. Scale bar, 500 μm. Reproduced with permission.<sup>72</sup> Copyright 2020, Spring Nature. (d) Microscopic robot with internal electronics fabricated by semiconductor techniques. Scale bar, 20 μm. Reproduced with permission.<sup>39</sup> Copyright 2020, Spring Nature.

precise motion control *via* logic circuits.<sup>10,39</sup> Miskin *et al.* developed a new class of mobile microrobots based on electrochemical actuation (Fig. 2(d)).<sup>39</sup> Due to the compatibility of manufacturing with silicon processing technology, thousands of microrobots can be obtained in a chip through the integrated process. When a laser is irradiated on the photovoltaics integrated on the microrobotic system, the robot's legs would deform, thereby allowing the robot to move. Moreover, Wang *et al.* proposed electrochemically actuated cilia metasurfaces that can be controlled by CMOS clock circuit to achieve arbitrary programmable flow pattern.<sup>10</sup> This kind of microrobotic system seamlessly integrating silicon processing and electronic control signals demonstrates an important advance in mass-fabricated and multifunctional intelligent microrobots.

### 3.2 Modular assembly based on self-healing and welding

Self-healing properties endow polymers with the ability to form interfacial connections, which facilitates the modular assembly of robotic structures.<sup>111–119</sup> A variety of dynamic covalent networks or non-covalent connection mechanisms have been developed to achieve self-healing properties, and the stable connections between interfaces are formed *via* temperature and light stimulation or automatically.<sup>117,119–121</sup> Fang *et al.* proposed a modular 4D printing strategy for the assembly of

heterogeneous deformable structures (Fig. 3(a)).<sup>41</sup> Shape memory structures containing dynamic covalent bonds were prepared by digital light processing (DLP) printing, and a crosslinking gradient was formed by controlling the exposure dose. The 2D films can be developed into 3D structures after solvent evaporation and form multilayer heterogeneous material architecture by interfacial welding (at a temperature environment of 70 °C). The constructed modular integrated structure can create sequential compression under a constant load and different temperature environments. The size of one assembly unit of the structure in Fig. 3(a) is about 10 mm which is comparable to the millimeter scale, and the size of the device after assembly is about 20–30 mm. The proposed fabrication method can be applied to the modular assembly of millimeter-scale robots with the increasing accuracy of 3D printing equipment. Therefore, it is of great significance for the development of small-scale integrated robots. Kuang *et al.* and Cheng *et al.* applied the self-healing property to magnetically actuated robotic systems, and the constructed magnetic soft robots were capable of rapid self-healing based on a dynamic Diels–Alder reaction and disulfide bond formation, respectively (Fig. 3(b) and (c)).<sup>40,122</sup> Using these magnetic dynamic polymers, soft robotic structures with different magnetization profiles can be purposefully assembled or reprogrammed to form reconfigurable soft robotic systems. Furthermore, Zhang *et al.* proposed a

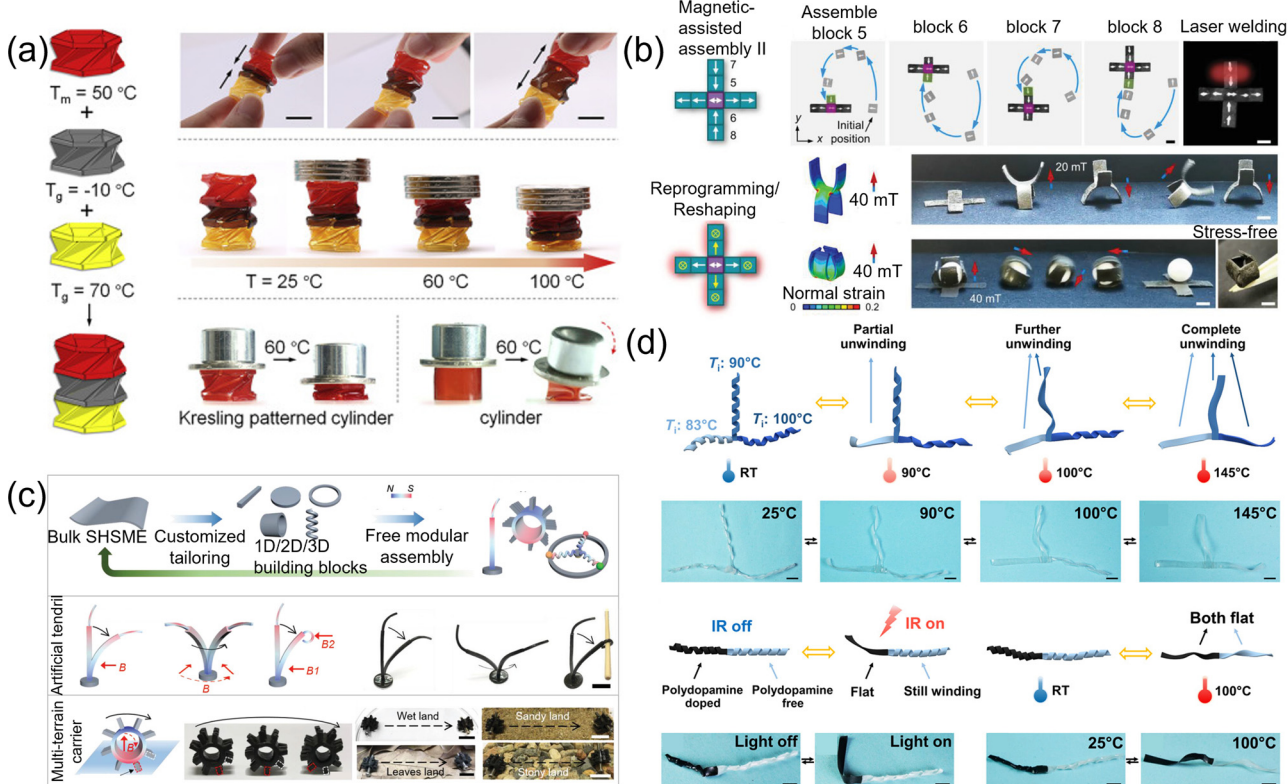


**Fig. 3** Modular assembly based on self-healing and welding. (a) Fabrication of multimaterial assembled Kresling origami structures using a modular 4D printing strategy for interfacial self-healing. The individual components of the origami structure have different glass transition temperatures. Scale bar, 10 mm. Reproduced with permission.<sup>41</sup> Copyright 2020, Elsevier. (b) Building a reprogrammable magnetically actuated soft robot with interfacial self-healing. Scale bar, 6 mm. Reproduced with permission.<sup>40</sup> Copyright 2021, Wiley. (c) Closed-loop modular assembly of a self-healing supramolecular magnetic elastomer to achieve diverse functionalities. Scale bar, 20 mm. Reproduced with permission.<sup>122</sup> Copyright 2021, Wiley. (d) Formation of multifunctional and multimaterial liquid crystal elastomer actuators via material welding to achieve sequential and area-selective responsive behaviors. Scale bar, 5 mm. Reproduced with permission.<sup>42</sup> Copyright 2020, American Association for the Advancement of Science.

weldable multicomponent LCE robot (Fig. 3(d)).<sup>42,123</sup> Acrylate groups were introduced into the LCE film to form permanent covalent bonds through thermal polymerization to ensure the stable welding of the film. The welding of LCE with different compositions *via* interfacial welding techniques enables robotic structures to selectively respond to light and heat in different regions.

### 3.3 Modular assembly based on bonding agents

Through the interaction between material interfaces or the introduction of bonding agents such as uncured materials, glues, and tapes, multifunctional soft robots can be fabricated in a bottom-up assembly.<sup>124,125</sup> For example, the LCE and the magneto-elastomer can form a stable interface connection during the curing process, and the interface toughness of the millimeter-scale double-layer elastomer structure could reach  $28 \text{ J m}^{-1}$ .<sup>126</sup> Through this interfacial connection, the bilayer elastomer material can form a complex dual-response deformation behavior under the action of heat and magnetic stimuli. To develop small-scale magnetic soft machines with arbitrary magnetization profiles and material compositions, Zhang *et al.* used uncured elastomers to connect heterogeneous micro-components (Fig. 4(a)).<sup>57</sup> Through two-photon lithography

printed micro-molds, these bonding agents can form surface connection or edge connection between skeleton modules and magnetic modules with different magnetization profiles. This assembly method shows great advantages in the construction of 3D miniaturized wireless actuated devices for biomedical applications such as soft capsules, peristaltic pump, and anchoring machine. In addition, Wu *et al.* assembled a magnetically actuated robot body with a biomimetic adhesion module through uncured ecoflex to construct a miniature soft robot with wireless climbing abilities (Fig. 4(b)). The assembled soft robot could move in complex pipes and porcine tissues *via* its unique footpad.<sup>127</sup> In addition, sprays have also been used to build stable interfacial connections. Yang *et al.* proposed a magnetic spray composed of poly(vinyl alcohol) (PVA), gluten, and magnetic particles (Fig. 4(c)).<sup>36</sup> When the spray adhered to inanimate objects, it was magnetized and solidified to form a magnetically actuated robot. It is worth mentioning that this magnetic coating can be decomposed under the action of an oscillating magnetic field. Although these assembly methods based on bonding agents have a high degree of freedom, they would increase the time and complexity required for manufacturing. To address this challenge, Dong *et al.* proposed multifunctional magnetic soft robots based on an adhesive sticker

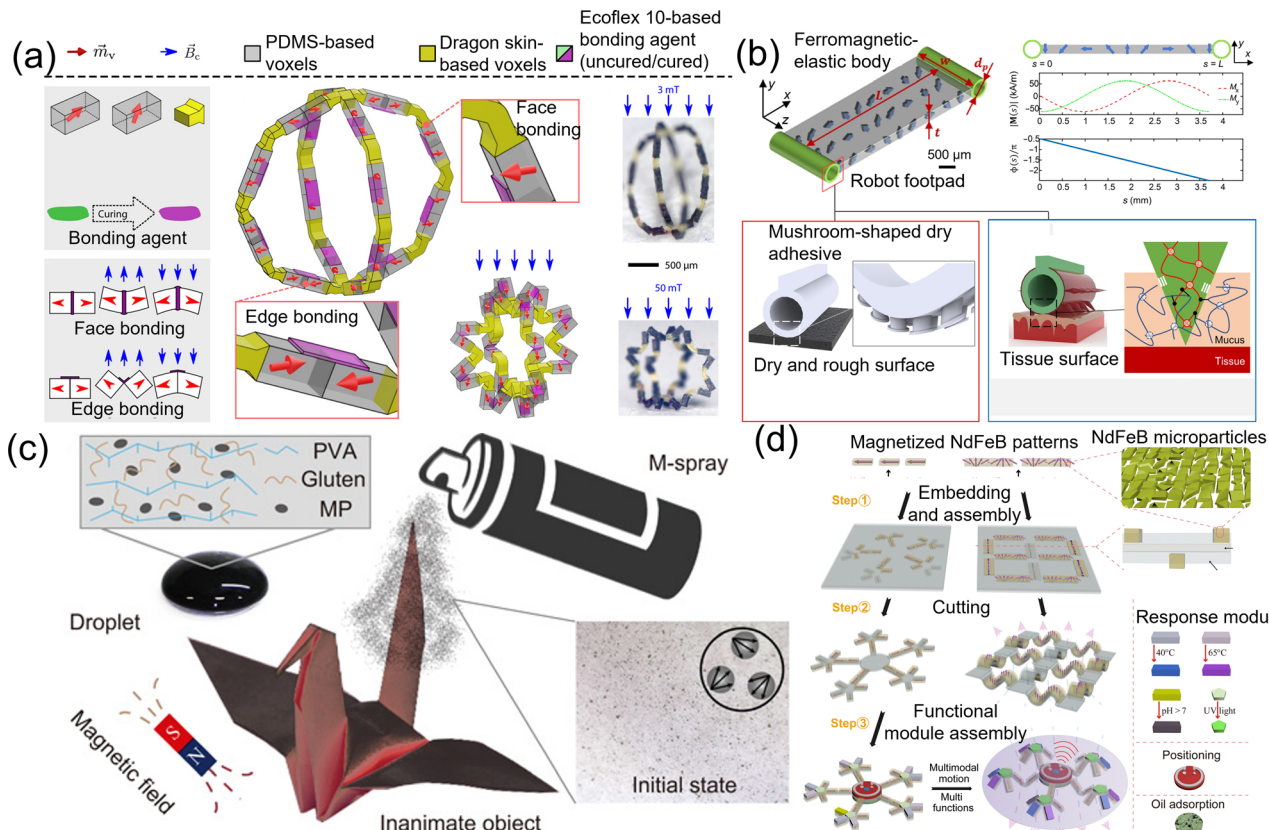


**Fig. 4** Module assembly based on bonding agents. (a) 3D soft magnetic machines with heterogeneous voxels constructed by micro jigs and bonding agents. Scale bar, 500  $\mu$ m. Reproduced with permission.<sup>57</sup> Copyright 2021, American Association for the Advancement of Science. (b) The two sides of the body of the magnetic drive robot are bonded with foot pads with an adhesive function to realize the climbing function in a closed and restricted space. Scale bar, 500  $\mu$ m. Reproduced with permission.<sup>127</sup> Copyright 2022, American Association for the Advancement of Science. (c) Droplets containing magnetic particles are sprayed onto inanimate objects to transform them into magnetic robots. Reproduced with permission.<sup>36</sup> Copyright 2020, American Association for the Advancement of Science. (d) Bonding of heterogeneously magnetized NdFeB patterns and various functional modules in a double-sided tape network. Reproduced with permission.<sup>37</sup> Copyright 2022, American Association for the Advancement of Science.

network (Fig. 4(d)).<sup>37</sup> Magnetic particles with different magnetization directions are transferred to the adhesive sticker to build a miniature machine with anisotropic magnetization profiles, and the adhesive property of the tape can also facilitate the integration of various functional modules, such as electronic components, oil absorption modules, and photosensitive modules.

### 3.4 Laser machining technique

Surface modification of the robot body can change the surface properties such as wettability and adhesion, allowing the selective integration with actuation units or other functional units.<sup>128–132</sup> For instance, Zhang *et al.* used a laser to micro-machine the surface of polydimethylsiloxane (PDMS) elastomers to form complex groove structures (Fig. 5(a)).<sup>43</sup> These microstructures can transform the PDMS surface from hydrophobic to hydrophilic. Furthermore, by introducing ferrofluid on the surface of these elastomers, the elastomers will exhibit 3D deformations due to the absorption of the solvent. After the evaporation of the solvent, the remaining magnetic particles will constitute the actuation unit of the robotic system. Other

functional units can also be loaded onto the robot by dispersing functional materials in the solvent. In addition, Ke *et al.* combined this selective adhesion property based on a surface modification strategy with transfer printing technology (Fig. 5(b)).<sup>133</sup> Elastomeric stamps with tunable adhesion properties were obtained by ablating with different laser parameters. This selective transfer printing strategy can be used to construct magnetic soft robots with a 3D discrete anisotropic magnetization profile, hierarchical structures, and the integration of functional units including thermally-responsive SMP, temperature sensor, and LED unit.

### 3.5 Template assisted method with a modular material design for multifunctional miniature robots

Smart materials are also called stimuli-responsive materials, and refer to a class of materials that can sense environmental stimuli and respond to changes.<sup>134–139</sup> Integrated robots based on smart materials exhibit higher levels of functionality and sophistication. Recent research innovations in smart materials provide broader opportunities and options for the fabrication and development of integrated robots. In addition, compared

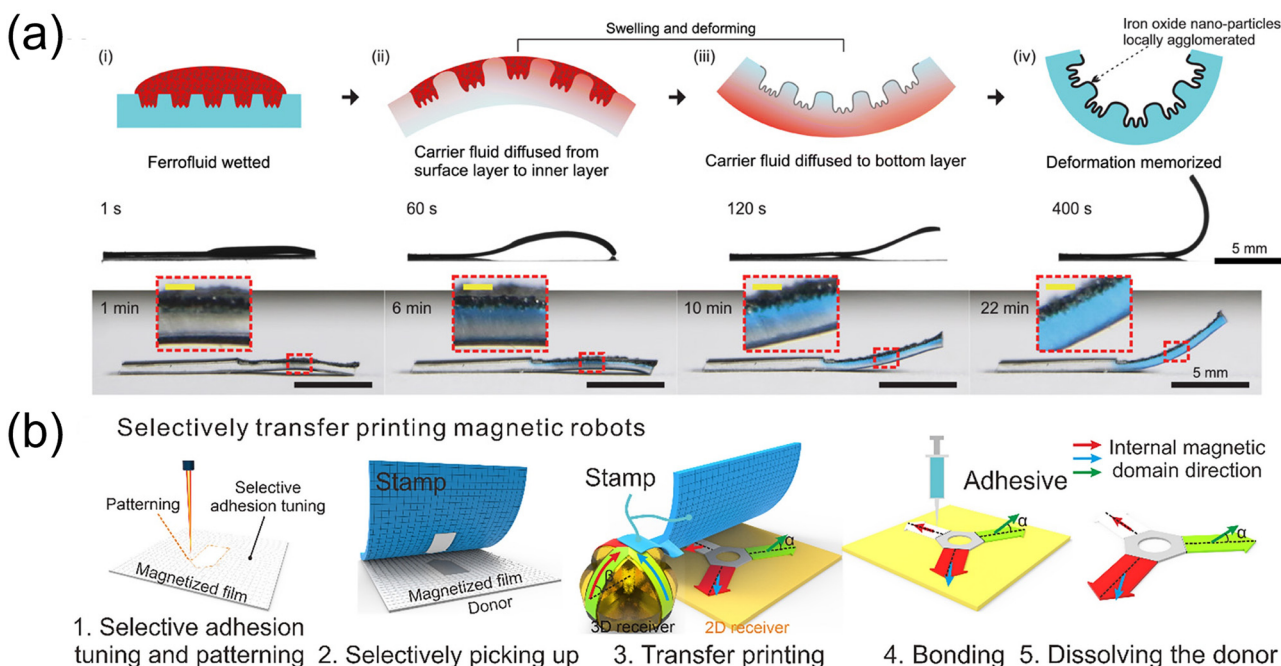


Fig. 5 Laser machining technique. (a) Schematic and experimental results of the deformation generated using a ferrofluid-infiltrated multifunctional elastomer sheet. The surface of the PDMS elastomer sheet is treated by selective laser scanning to make the surface hydrophilic. Scale bar, 5 mm. Reproduced with permission.<sup>43</sup> Copyright 2021, American Association for the Advancement of Science. (b) Fabrication of multifunctional soft magnetic robots via selective transfer printing. Reproduced with permission.<sup>133</sup> Copyright 2021, Elsevier.

with traditional rigid and electrically driven robots, integrated robots based on stimuli-responsive materials are more promising to overcome the microscopic conditions caused by scaling effects, such as friction, fluid force, *etc.* Moreover, the integrated miniature robots based on stimuli-responsive materials also show broader application prospects due to the programmable form of movement and modular body structure design. In recent years, a variety of integrated miniature robots based on smart materials have been reported, which can sense different environmental stimuli, such as light, acoustic wave, electronic, magnetic, heat and chemical stimuli, and generate responsive behaviors, such as motion, deformation, or colour change. For instance, Wang *et al.* reported a chemical-responsive soft actuator based on the fast vapor-absorbing/desorbing capabilities of poly(trimethylolpropane triacrylate) (PTMPTA) (Fig. 6(a)).<sup>104</sup> Specifically, this smart actuator exhibited the color shifting and shape transformation abilities when sensing solvent stimuli, such as ethylene glycol (EG), *N,N*-dimethylformamide (DMF), water, ethanol, acetone, and chloroform. Through the coordination of vapochromic and vapomechanical responses, the structural-color films exhibited a variety of integrated response behaviors and potential applications in the field of environment interaction. In addition, by combining photo/thermal actuation and piezoresistive sensing into a monolithic smart hydrogel material, Zhao *et al.* realized an octopi-inspired actuator that can simultaneously have optimum strain sensitivity and deformability without the attenuation of conductivity and mechanical robustness (Fig. 6(b)).<sup>44</sup>

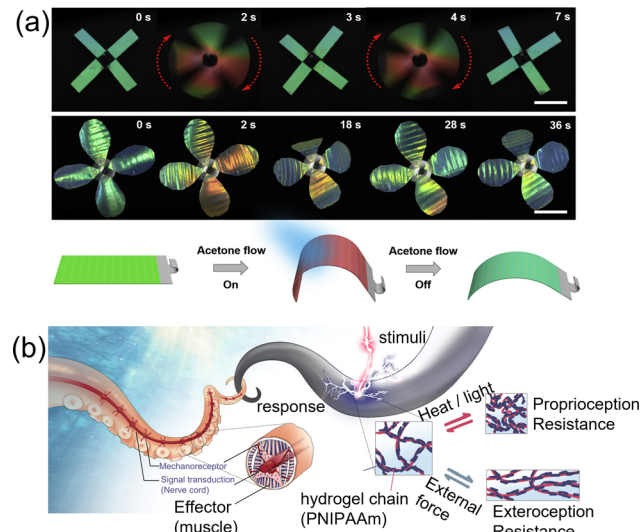


Fig. 6 Template assisted method with modular material design for multi-functional miniature robots. (a) Chameleon inspired actuator could generate locomotion and color change under acetone flow. Scale bar, 10 mm. Reproduced with permission.<sup>104</sup> Copyright 2019, Elsevier. (b) Schematic illustration of molecular design of conductive photothermally responsive hydrogel based bioinspired self-sensing actuator. Reproduced with permission.<sup>44</sup> Copyright 2021, American Association for the Advancement of Science.

Furthermore, they demonstrated the potential to prepare the self-diagnostic feedback-controlled autonomy miniature robot based on modular smart material design.

Variable stiffness materials enable soft robots to switch between a load-bearing state and a compliant state, and they have important applications in engineering fields such as minimally invasive surgery and prosthetics. Stiffness-variable polymers (SMP, LCE, dielectric elastomers), low melting point alloys, liquid metals, magnetorheological fluids, electrorheological fluids, and paraffin, have been applied to construct machines whose stiffness can be tuned by pressure, temperature, electric field and magnetic field.<sup>140</sup> The phase transition of magnetorheological and electrorheological fluids is dependent on the viscosity of the filler material and cannot withstand tensile or bending loads. The phase transition of polymers is susceptible to retardation. To cope with the limitations, Wei *et al.* proposed a variable stiffness robotic gripper based on pneumatic actuators and particle jamming.<sup>141</sup> The particles are loosely wrapped in an elastic membrane, forming a soft structure in the natural state, and the particles are firmly stacked in the membrane in a vacuum state, which can achieve a stiffness enhancement of more than 10 times, making the soft robotic gripper with an adaptive grasping capability. Using particle jamming to achieve a fast reversible phase transition, the delay time can reach  $\sim 1$  s. Stiffness-variable structures based on particle jamming cannot resist significant tensile stress. Jadhav *et al.* employed fiber jamming which consists of axially encapsulated fibers to achieve widely tunable bending stiffness.<sup>142</sup> In the free state, the structure is compliant along the longitudinal direction, and in the vacuum state, the increased friction between the fibers results in a significant increase in the rigidity of the structure. Fiber jamming structures have the ability to withstand a variety of loading conditions, such as high bending and buckling loads. Fiber jamming based variable stiffness devices are used in force-feedback haptic gloves that can grasp objects in augmented reality. Ha *et al.* manipulated the spatial distribution of micro-water molecules in poly(acrylamide/2-acrylamido-2-methylpropane sulfonic acid) through the phase transition of supersaturated sodium acetate trihydrate, enabling the structure to switch between a homogeneous soft state and a heterogeneous rigid state.<sup>143</sup> The structural stiffness was able to fluctuate between 110 kPa and 1.09 GPa through thermal stimulation and chemical perturbation.

### 3.6 3D printing techniques

The development of 3D printing technologies, especially multi-material 3D printing technology, has provided promising technology for the development of multifunctional soft robots.<sup>144–153</sup> Currently, direct ink writing (DIW), two photon polymerization (TPP), DLP printing technologies have been extended to multi-material printing, and widely used in the preparation of soft robots. Different soft and rigid materials, hydrogel and elastomeric materials, responsive and non-responsive materials can be integrated by multi-material printing technologies.<sup>45,154,155</sup> For example, Skylar-Scott *et al.* used multi-nozzle 3D printing technology to print silicon polymers with different stiffnesses and build soft-bodied pneumatic soft-bodied walking robots (Fig. 7(a)).<sup>45</sup> To develop artificial

musculoskeletal systems at a microscale, Ma and co-workers proposed a multimaterial femtosecond laser printing strategy (Fig. 7(b)).<sup>155</sup> The printable polymers, including the rigid SU-8 resin used for skeleton structure and pH-responsive bovine serum albumin used for muscle structure, are successively injected into the polymerization chamber and removed on demand. The printed artificial musculoskeletal system ( $\sim 30$   $\mu\text{m}$  side length) could precisely capture a microcube (10  $\mu\text{m}$  side length) *via* pH stimuli. In addition, through the embedded 3D printing technology, the somatosensory sensing unit (multiple soft sensors) and the actuation units can be integrated, and the robot could recognize different manipulated objects during the actuation process according to the feedback of the robot's electrical resistance (Fig. 7(c)).<sup>156</sup> Hybrid structures composed of hydrogels and elastomers or rigid polymers could lubricate biomedical devices and reinforce hydrogel-based flexible devices. However, interfacial delamination is prone to occur between hydrogels and other polymers, and it is difficult to construct precise 3D composite structures. Ge *et al.* proposed a DLP-based multi-material 3D printing technology to form covalent bonding of hydrogels with other photocurable polymers through incomplete polymerization of water-soluble initiators (Fig. 7(d)).<sup>154</sup> This fabrication method shows a variety of applications, including shape-memory cardiovascular stents and pneumatic grippers integrated with hydrogel strain sensors. Combining multi-material 3D printing technology with topological metamaterial structures could greatly expand the structural design and shape-morphing capabilities of soft robots. Cui *et al.* printed 3D lattice structures through multi-material stereolithography and integrated conductive, piezoelectric and structural modules within them (Fig. 7(e)).<sup>157</sup> The responsiveness of piezoelectric materials enables robotic superstructures to achieve different locomotion modes (walking, jumping, steering) and an active sensing capability (e.g., obstacle avoidance).

4D printing technique adds a fourth dimension – time – to the 3D structure, so that the printed structure can change its shape or function under external stimuli. The programming of physical properties of fillers in composite materials, the control of filler orientation, or the degree of crosslinking density of polymer networks have been developed for 4D printing methods.<sup>21,27,158,159</sup> A variety of printable composite materials and stimuli-responsive materials (hydrogels, LCE, SMP) have been proposed. For example, Ma *et al.* used pH-responsive bovine serum albumin to print an artificial musculoskeletal system, and the structure could be folded and unfolded according to changes in environmental pH.<sup>155</sup> Fang *et al.* controlled the crosslinking density gradient of the dynamic crosslinked polymer by adjusting the exposure time.<sup>41</sup> After printing, the 2D film structure will be transformed into a 3D geometric shape with the removal of the solvent. Furthermore, the interface welding ability of the dynamic polymer is used to assemble the printed structures, enabling more complex multi-layer 3D geometry transformations, and providing a modular 4D printing platform.

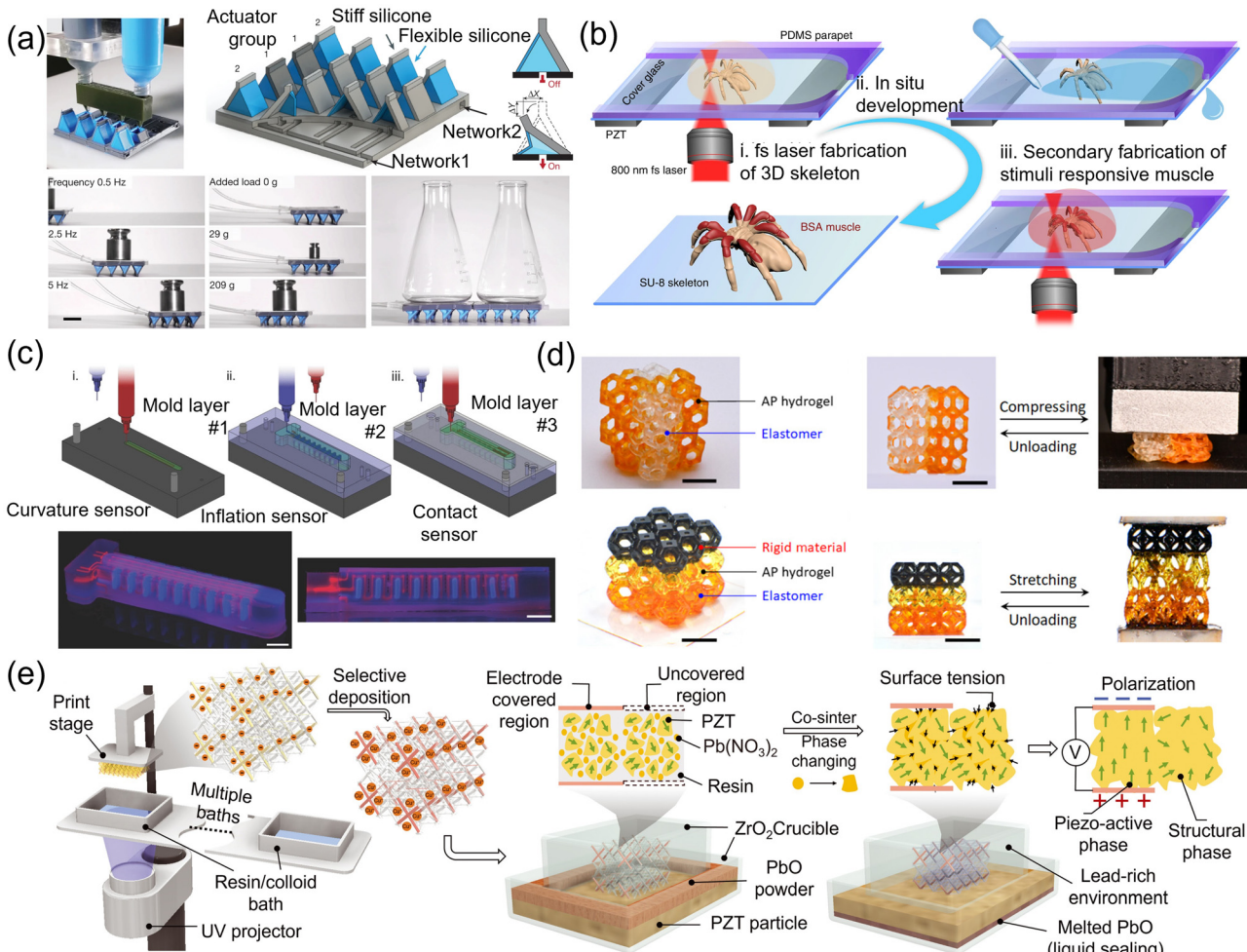


**Fig. 7** 3D printing techniques. (a) Multi-nozzle DIW printing technology for the preparation of pneumatic walking robots integrating materials with different stiffness. Scale bar, 20 mm. Reproduced with permission.<sup>45</sup> Copyright 2019, Spring Nature. (b) Continuous two-photon printing technology builds complex 3D robotic structures fused with heterogeneous materials. Reproduced with permission.<sup>155</sup> Copyright 2020, Spring Nature. (c) Embedded 3D printing technology used for the directly preparing a pneumatic gripper with both sensing and actuation capabilities. Scale bar, 10 mm. Reproduced with permission.<sup>156</sup> Copyright 2018, Wiley. (d) DLP-based multimaterial 3D printing technology builds 3D foam structures consisting of rigid polymer, hydrogel, and elastomer. Scale bar, 5 mm. Reproduced with permission.<sup>154</sup> Copyright 2021, American Association for the Advancement of Science. (e) The robotic metamaterial structure is prepared based on DLP multi-material printing technology, which has a structural phase, conductive phase, and piezo-active phase at the same time. Reproduced with permission.<sup>157</sup> Copyright 2022, American Association for the Advancement of Science.

## 4. Applications of multicomponent and multifunctional integrated miniature soft robots

With the seamless integration of functional units, the integrated design and fabrication strategies provide a platform technology to endow miniature soft robots with a broad range of applications. The integrated robotic system could load different types of functional units or utilize the reconfigurability of modules to replace functional units to achieve multi-task execution, which is difficult for a single-component robotic system. In this section, we deliver recent advances in MIMSRs in terms of engineering applications, including biomedical applications, environmental and proprioceptive sensing, and intelligent electronics.

### 4.1 Biomedical application

Medical catheter and guidewire technology place an important role in minimally invasive surgery which could reduce surgical risks and shorten recovery times.<sup>160–170</sup> The catheter-based interventions have a wide range of applications in the treatment of cardiovascular diseases.<sup>6,100,164</sup> In addition to delivering the catheter to the designated location, a variety of challenging tasks need to be accomplished, such as monitoring physiological environment (electrophysiological parameters, temperature, and pressure, *etc*), applying electrical or thermal stimulation to soft tissue, delivering therapeutic drugs and cells, embolization and clot removal. Based on these requirements, a variety of functional components are integrated into the catheter structure, such as manipulator tools and soft sensors, which may impede the miniaturization of

multifunctional integrated catheters and hinder their applications in narrow and tortuous vasculatures. Semiconductor processing technology provides a feasible solution for the integration and miniaturization of medical catheters. Rivkin *et al.* utilized the self-rolling process to fabricate a hollow microcatheter (0.1 mm in diameter) integrated with an electrically actuated gripper and magnetic sensor (Fig. 8(a)).<sup>109</sup> The integrated catheter can be moved in a curved channel with a diameter of only 0.2 mm, and the hollow structure can be used to deliver fluids in the esophagus and stomach of a mouse. A gripper actuated by a conductive polymer film integrated at the end of the catheter is able to capture particles with a diameter of 0.1 mm in a tube, which is expected to be used to capture

blood clots or cells. Finally, the magnetic sensor occupies the function for *in vivo* localization and navigation of the microcatheter, which can utilize the anisotropic magnetoresistive effect to detect changes in the magnetic field in space and reach a resolution of 0.1 mm. Different from Rivkin *et al.* who fabricated microcatheters, Han *et al.* directly integrated multiplex flexible electronics and actuators on a commercialized catheter (Fig. 8(b)).<sup>100</sup> The lateral dimension of the electronic equipment covered on the catheter is about 1 cm, including an electrode array with electrophysiology measurement and electrical stimulation functions, temperature sensor array, and pressure sensor array. These flexible electronic arrays can withstand the inflation and deflation of the balloon on the

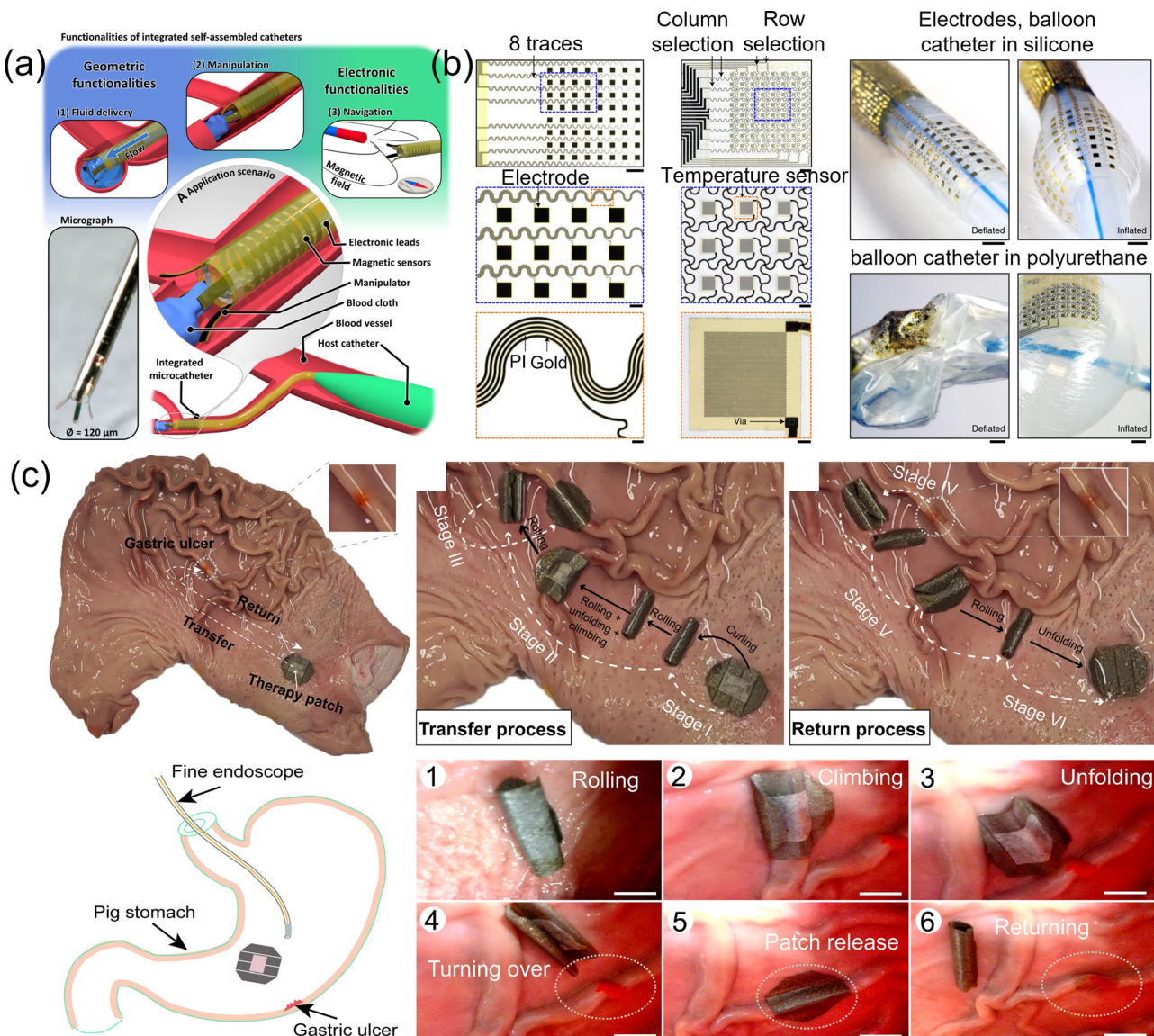


Fig. 8 Biomedical application. (a) Functionalities and application scenario of integrated self-assembled catheters. Reproduced with permission.<sup>109</sup> Copyright 2021, American Association for the Advancement of Science. (b) Silicone balloon catheter integrating vertically stacked temperature sensor array, pressure sensor array, and electrode array. Reproduced with permission.<sup>100</sup> Copyright 2020, Spring Nature. Scale bar, 2 mm. (c) Soft robot actuated in the stomach to transfer therapy patch and cover gastric ulcer. Scale bar, 10 mm. Reproduced with permission.<sup>37</sup> Copyright 2022, American Association for the Advancement of Science.

catheter, and 10 000 cycles of uniaxial stretching. Selective powering of electrode arrays facilitates programmable radio-frequency ablation (heating tissue) and irreversible electroporation (increasing cell permeability and leading to local cell death) for the treatment of arrhythmias. Integrated pressure sensors can simultaneously monitor ventricular action for surgical improvement.

Wirelessly actuated microrobots have broad application prospects in precision medicine such as targeted drug delivery and cell delivery.<sup>49,50,87,171–176</sup> For the targeted delivery application, miniature soft robots integrated with therapeutic units (such as components loaded with cells or drugs) have been developed. For example, Zhang *et al.* proposed an anchoring device that assembled different magnetized units into a three-dimensional lattice structure, that can shrink and restore its radial dimension under the action of a magnetic field, thereby realizing the release and anchoring functions.<sup>57</sup> There are TPP printed cell cages in the anchoring device used as a cell scaffold to carry stem cells. The carried stem cells could proliferate, migrate and differentiate cells after reaching the designated position, which is expected to achieve medical applications such as vascular regeneration. There is a key issue in microrobot-based targeted delivery, that is, how to separate from the therapeutic units and retrieve the robot body after the robot carrying the therapeutic units reaching the target location. To address this issue, Dong *et al.* proposed a magnetically actuated multifunctional soft robot based on an adhesive sticker network (Fig. 8(c)).<sup>37</sup> Magnetic units with different 3D magnetization profiles can be integrated into the soft robot by using the adhesive sticker. A therapy patch used for gastric ulcer treatment was integrated into the robot body *via* soluble tape. During the locomotion of the robot, the therapy patch is wrapped in the robot to avoid the influence of gastric fluids. The therapy patch would be released due to the dissolution of the soluble tape in gastric mucosa when the robot moves to a gastric ulcer, demonstrating its application potential in gastric ulcer treatment.

#### 4.2 Environmental and proprioceptive sensing

Organisms can sense their surrounding physical environment and their own movements to adapt to the environment. In order to endow soft robots with intelligence inspired by biological systems, researchers have developed a variety of robotic systems that combine perception and actuation capabilities to achieve closed-loop control of locomotion and enhance their functionality.<sup>177–182</sup> First of all, miniature soft robots could load functional units to achieve environmental sensing. For instance, Dong *et al.* proposed a simple strategy for seamless integration of various environment perception modules into soft robotic systems (Fig. 9(a)).<sup>37</sup> As a proof-of-concept, temperature, UV sensing particles, and pH sensing paper are incorporated into the adhesive sticker. The repeatability of the stickers allows these sensor modules to be easily replaced after use. Zhang *et al.* utilized a laser scanned PDMS sheet to selectively absorb quantum dot solutions, photosensitive ink, and thermochromic ink in different regions (Fig. 9(b)).<sup>43</sup>

A frog-inspired origami robot was fabricated with this integration strategy which could switch skin color in response to the variation of thermal and optical environment.

In addition to the environmental sensing, the integration of the proprioception and actuation units of a soft robotic system is also a challenge leading to the construction of a biomimetic neuromuscular drive system. Some somatosensory sensors have been developed, which can monitor the roughness of manipulated objects and various types of deformation (Fig. 9(c) and (d)). A somatosensitive pneumatic actuator integrated with multiple soft sensors including curvature sensor, inflation sensor, and contact sensor was fabricated by multi-material embedded 3D printing (Fig. 9(c)).<sup>156</sup> Different resistance changes of the soft sensors are generated during the upward bending, downward bending, and flicking of the robotic gripper, which provide the desired somatosensory feedback. Furthermore, the pneumatic gripper can sense the surface texture and temperature of the object being grasped due to the change of the contact pressure when grasping objects with different surface roughness and the change of the local conductivity caused by objects with different surface temperatures. Zhao *et al.* proposed a hydrogel material system consisting of an interpenetrating double network of thermally responsive pNIPAm and conductive polyaniline (PAni) (Fig. 9(d)).<sup>44</sup> This polymer network structure enables seamless integration of photothermal actuation and piezoresistive sensing. This hydrogel soft robot can rapidly respond to the stimulation of near-infrared light to generate structure contraction, expansion, and bending. Meanwhile, due to its own electronic conduction characteristics, the robot can perceive the external force or the structural deformation generated by infrared light stimulation through the variation of resistance. Therefore, the developed somatosensory soft robot is able to recognize the manipulated unknown object and employ a closed-loop control algorithm to manage the task execution.

Organisms such as flowers, chameleons, octopuses, cuttlefish, squid, and frogs, can actively change color to protect themselves or increase their chances of predation.<sup>178,183</sup> Giving the soft robot the color-changing function can expand its artificial camouflage ability and active environmental monitoring ability. Inspired by natural organisms, a variety of mechanisms have been explored to construct active color-changing soft robots, including thermochromic, mechanochromic, electrochromic, thermochromic, photochromic and other principles, and a variety of color-changing materials have been developed, including thermochromic liquid crystal inks, superparamagnetic nanoparticles, hydrogels and polymer films with inverse opal structures. Kim *et al.* combined a thermochromic liquid crystal ink with multilayer silver nanowire heaters.<sup>184</sup> Different numbers of silver nanowire heaters are formed according to the changes in the target microenvironment. The color of the thermochromic ink depends on the surface temperature, and the regulation can be achieved by changing the applied voltage or the concentration of silver nanowires. Using the feedback system based on PID control, the surface temperature can be actively modulated to stably display the specified color,

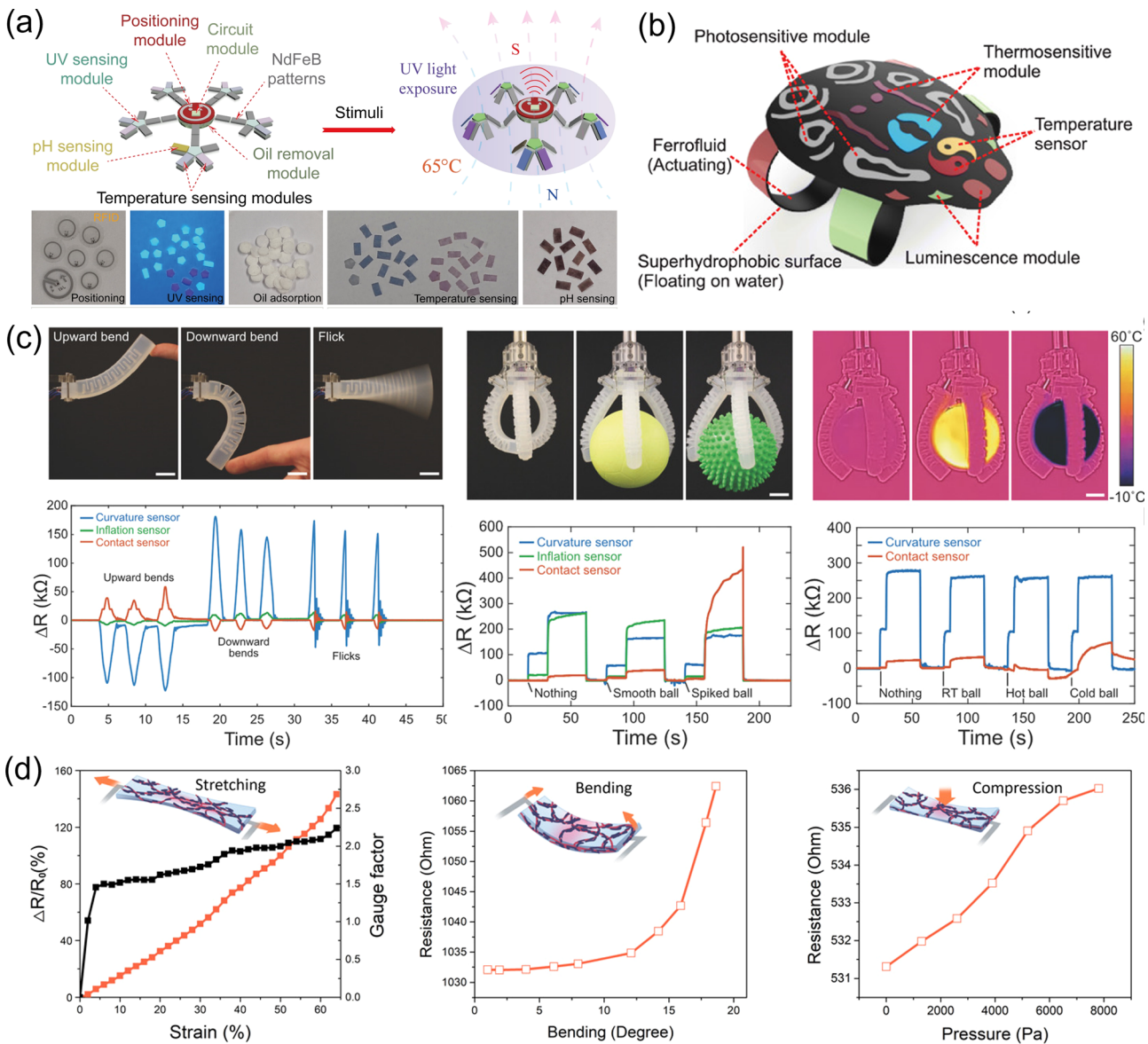


**Fig. 9** Environmental and proprioceptive sensing. (a) Schematic illustration and optical images of functional modules of multifunctional multilegged soft robot. Reproduced with permission.<sup>37</sup> Copyright 2022, American Association for the Advancement of Science. (b) Schematic illustration of a frog-like multifunctional soft robot and demonstration of its switchable coloration under different circumstances. Reproduced with permission.<sup>43</sup> Copyright 2021, American Association for the Advancement of Science. (c) 3D printed pneumatic actuator integrated with somatosensitive sensor. Scale bar, 20 mm. Reproduced with permission.<sup>156</sup> Copyright 2018, Wiley. (d) Resistance changes of responsive hydrogel under stretching, bending, and compression. Reproduced with permission.<sup>44</sup> Copyright 2021, American Association for the Advancement of Science.

reducing the influence of the ambient temperature. Kim *et al.* used silver nanowire networks, transparent polymer films, and color-changing inks to construct biomimetic soft actuators with color-changing functions.<sup>183</sup> Applying a voltage through the silver nanowire network to generate heat causes the polymer film to bend and produce a change in surface color. Using the anisotropic deformation characteristics and temperature-dependent color change properties of polymer films, soft actuators such as blooming flowers and winding tendrils that mimic organisms can be constructed. Inspired by cephalopods, Lee *et al.* developed a skin-based device that utilizes thermoelectric units for stealth in the visible and infrared regions.<sup>185</sup>

The thermoelectric unit is conducive to precise temperature tunability. In addition, by introducing thermochromic liquid crystals, a variety of colors could be generated by adjusting the temperature, thereby achieving stealth in the visible light range. The constructed thermal display mounted on the human epidermis can provide a multispectral stealth system, which has high practicability for wearable military applications.

In addition to color changes, transparent structures are also adopted by a variety of organisms, such as eel, jellyfish, and glasswing butterfly, to achieve camouflage.<sup>186</sup> Biomimetic transparent robots could avoid the mismatch with background colour and are suitable for almost all environments. Various

advanced materials, including transparent dielectric elastomers, PDMS, hydrogels, and low-density polyethylene, have been developed to fabricate imperceptible structures. Christianson *et al.* developed a jellyfish-inspired swimming robot actuated by fluid electrode dielectric organic actuators.<sup>187</sup> Acrylic elastomer was used as the dielectric layer of the actuator allowing the silent and stealthy locomotion of the robot at the speed of  $3.2 \text{ mm s}^{-1}$ . In addition, Li *et al.* developed a transparent soft robot based on a transparent dielectric elastomer actuator, which has a transmittance of more than 80% and is capable of exhibiting a large voltage-induced area strain of 200%.<sup>188</sup> The developed transparent actuator could switch between 3D shapes and 2D structures by tuning the voltage and simultaneously achieve effective camouflage in dynamic or unstructured environments. Besides the dielectric elastomer, Lee *et al.* developed a transparent actuator based on a three-layer composite material, including silver nanowire networks, low-density polyethylene, and polyvinyl chloride layers.<sup>189</sup> As a transparent heater, the silver nanowire network could induce the deformation of low-density polyethylene and polyvinyl chloride films. The soft actuator has good controllability of bending direction and can be applied to transparent grippers and walking robots with a low operating temperature ( $40^\circ\text{C}$ ).

#### 4.3 Intelligent electronics

The integration of miniature soft robots and electronic components is of great significance for the construction of reconfigurable electronic devices including logic circuits and morphable

antennas. Kim *et al.* combined a soft electronic circuitry and annular-ring shaped magnetic film with heterogeneous magnetization profiles. Two deformation modes would be induced by the external magnetic stimuli and different micro-LEDs lit up due to the selective contact of the electrode.<sup>27</sup> The connection modes of reconfigurable circuits produced by the magnetic films are limited by their transformation modes. To achieve multiple shape transformations, Ze *et al.* developed a magnetic SMP that could exhibit tunable stiffness *via* the heat generated by a high-frequency magnetic field and different deformability under the actuation magnetic field (Fig. 10(a)).<sup>68</sup> These magnetic SMP-based robots are applied to sequential digital logic circuits, with a high-frequency magnetic field and an actuation magnetic field as the input, and the on or off states of an LED as the output, which could realize logical functions including D-latch and three-bit memory. Apart from the thin-film structure-based logic circuit, more complex three-dimensional origami structures can also be used to build logic circuits. Novelino *et al.* adopted the Kresling origami structure in which magnetic discs with different magnetization directions and conductive components were integrated (Fig. 10(b)).<sup>190</sup> Under magnetic stimuli, the origami structure exhibits bistable stables including deployed and folded states which lead to the connection of different circuits and light up different colored LEDs. By assembling three Kresling origami structures, the integrated robotic system demonstrates its capability of digital computing of three-bit information. Antennas with dynamic shape-morphing capabilities could achieve reconfigurable

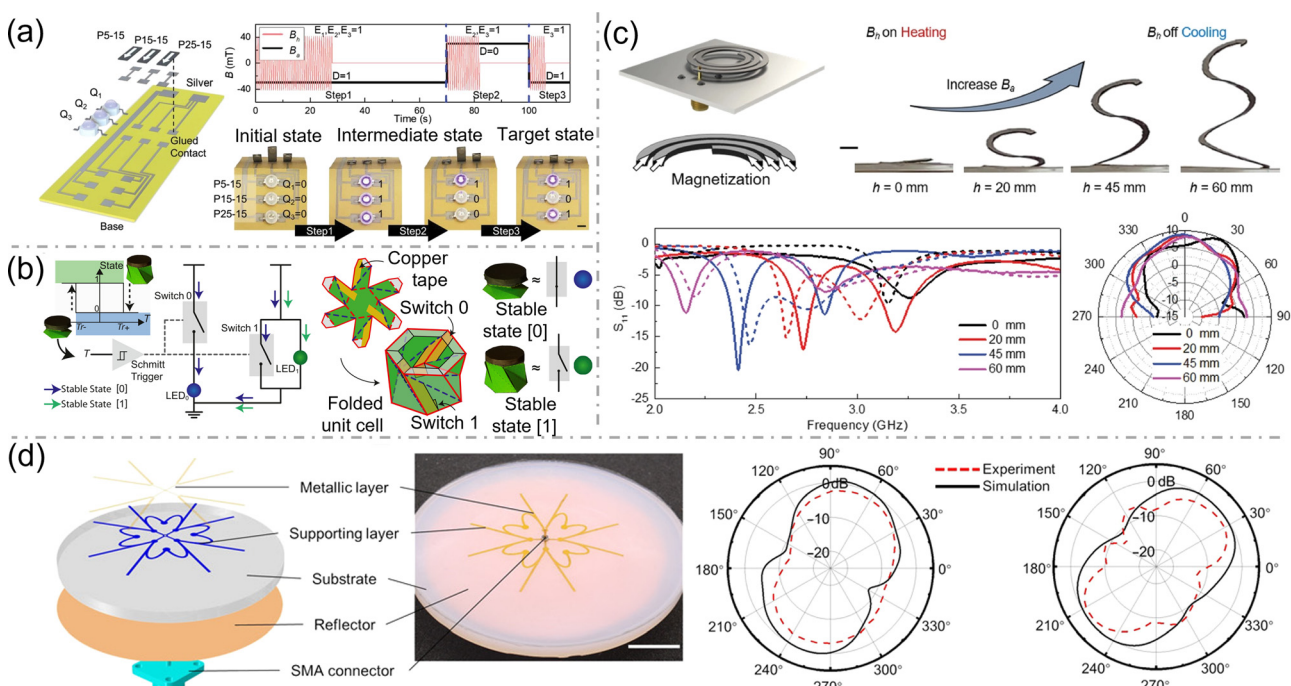


Fig. 10 Intelligent electronics. (a) Sequentially actuated robotic system for digital logic circuits. Scale bar, 5 mm. Reproduced with permission.<sup>68</sup> Copyright 2020, Wiley. (b) Logic circuit based on magnetic actuated Kresling origami. Reproduced with permission.<sup>190</sup> Copyright 2020, National Academy of Sciences. (c) Actuation results, S<sub>11</sub> band results, and 2D polar plot of the morphing helical antenna. Scale bar, 5 mm. Reproduced with permission.<sup>68</sup> Copyright 2020, Wiley. (d) The schematic illustration, images, and radiation pattern for the reconfigurable multimodal antenna. Scale bar, 20 mm. Reproduced with permission.<sup>191</sup> Copyright 2020, American Association for the Advancement of Science.

frequency response properties. Ze *et al.* designed a tapered helical antenna based on a magnetic SMP, which could exhibit a controllable deformation height actuated by an external magnetic field (Fig. 10(c)).<sup>68</sup> The resonant frequency of this reconfigurable antenna can be tuned between 2.15 and 3.26 GHz, and the structure can be locked *via* the shape memory property of the antenna. In addition, Bai *et al.* proposed a 3D reconfigurable antenna based on buckling-guided assembly (Fig. 10(d)).<sup>191</sup> The sequential release of the pre-strain of the elastic substrate can induce multiple deformation modes of the 3D structure. The developed Antennas with this strategy can switch between 9 shape morphing modes, exhibiting widely tuneable radiation directions.

Stimuli-responsive materials, such as inorganic carbon materials, metal nanomaterials, SMP, and LCE, are of great significance for the development of intelligent actuators, flexible electronics, and wearable devices. For example, silver (Ag) nanowires with high electrical conductivity and aspect ratio can form stretchable and optically transparent films. Under voltage stimulation, the Ag nanowire network generates Joule heating which could promote bending deformation of polymer films and color shift of thermochromic materials.<sup>192</sup> Ag nanowire networks can be embedded into low-density polyethylene films, PDMS, polyimide films, and poly(3,4-ethylenedioxothiophene) polystyrenesulfonate thin layers to achieve efficient electrothermal actuation of robotic structures. Shape memory materials are a class of stimuli-responsive materials that can undergo a transition from glassy to rubbery state under thermal stimulation, resulting in changes in stiffness. The shape transformation capability of shape memory materials has broad application prospects in the fields of flexible electronics and soft robotics.<sup>193,194</sup> 2D shape memory films integrated with electronic components such as light-emitting diodes and microelectrode sensors are transferred onto pre-stretched elastomer substrates. Mechanical buckling strategies are adopted to form 3D SMP films and reformulate flexible electronics into 3D shapes. The 3D electronic devices could exhibit various temporary shapes due to the shape memory effect, and have been applied to the sensing of temperature, stiffness, and contact force. In addition, living cells provide a unique strategy to modulate the shape change of active materials based on their response to cues in biological environments. Rivera-Tarazona *et al.* synthesized hydrogel composites embedded with Baker's yeast whose proliferation leads to a controllable increase in the volume of composites.<sup>195</sup> The developed hydrogel composites are genetically manipulated to produce higher volume changes under specific amino acids. Combined with optogenetic coding, spatiotemporally controlled shape changes can be achieved. Cai *et al.* reported a multi-response actuator with MXene-cellulose composites and polycarbonate membranes to mimic the complex structure of leaves.<sup>196</sup> The developed actuator is capable of harvesting electrical and light energy and converting it to thermal energy, and rapidly exhibits programmable deformation under near-infrared light stimulation. The actuator, as a conductor, was used in near-infrared light-controlled smart switches. Once bending, the actuator could connect circuits under the irradiation of near-infrared light, and realize power supply to a smart watch.

## Conclusions and perspectives

This review delivers recent progress in multicomponent and multifunctional integrated miniature soft robots in terms of their integration strategies and applications. Representative actuation units, functional units, and their integration strategies are summarized. Their emerging applications in minimally invasive surgery, precision medicine, proprioceptive sensing, and intelligent electronics are discussed. The seamless integration of diverse actuation units and functional units greatly enhances the functionalities and adaptability of the miniature soft robots. While this field has progressed remarkably in recent years, further efforts are still needed to enhance the intelligence and reconfigurability of integrated miniature robotic systems.

Improving the intelligence of miniaturized soft robots so that they could learn and adapt to unstructured and real-world environments would be particularly attractive.<sup>136,137</sup> To develop intelligent miniaturized soft robots, it is necessary to improve their own reconfigurability and decision-making capabilities. The functional units and actuation units of integrated miniature soft robots are often fixed during preparation, which limits their reconfigurability. New smart materials and integration strategies need to be developed to improve the reconfigurability of miniature robotic systems, such as real-time reprogrammable actuation units, rapidly degradable bonding agents, and reprocessable robotic bodies. In addition, miniature soft robotic systems with loosely coupled interactions, such as self-assembly based on capillary force, dielectrophoretic forces or weak magnetic interactions, promise benefits in the high reconfigurability of morphology, behavior, and function of robotic systems.<sup>197–200</sup> Finally, the introduction of computational intelligence into the control strategies of a soft robotic system for autonomous adaption of each unit or their locomotion modes to the changing of an operation environment enables an appropriate decision-making ability for unknown and unstructured environments.<sup>201,202</sup>

## Abbreviations

CMOS	Complementary metal–oxide–semiconductor
DIW	Direct ink writing
DLP	Digital light processing
LCE	Liquid crystal elastomer
PDMS	Polydimethylsiloxane
pNIPAM	Poly( <i>N</i> -isopropylacrylamide)
PVA	Poly(vinyl alcohol)
SMP	Shape memory polymer
TPP	Two photon polymerization

## Author contributions

Conceptualization: N. X, G. Z, and Y. D. Writing – original draft: N. X. Writing – review & editing: L. Z, N. X, G. Z, X. W, and Y. D. Funding acquisition: L. Z. Supervision: L. Z.

## Conflicts of interest

There are no conflicts to declare.

## Acknowledgements

The research work is financially supported by the Hong Kong Research Grants Council (RGC) with project No. JLFS/E-402/18, C1134-20GF, and RFS2122-4S03, the Croucher Foundation Grant with Ref. No. CAS20403, and the CUHK internal grants. We also acknowledge the support from Multi-scale Medical Robotics Centre (MRC), InnoHK, at the Hong Kong Science Park, and the CUHK-SIAT Joint Research Laboratory on Robotics and Intelligent Systems.

## Notes and references

- 1 M. Wehner, R. L. Truby, D. J. Fitzgerald, B. Mosadegh, G. M. Whitesides, J. A. Lewis and R. J. Wood, *Nature*, 2016, **536**, 451–455.
- 2 B. H. Kim, K. Li, J.-T. Kim, Y. Park, H. Jang, X. Wang, Z. Xie, S. M. Won, H.-J. Yoon and G. Lee, *Nature*, 2021, **597**, 503–510.
- 3 M. Han, X. Guo, X. Chen, C. Liang, H. Zhao, Q. Zhang, W. Bai, F. Zhang, H. Wei and C. Wu, *Sci. Rob.*, 2022, **7**, eabn0602.
- 4 Z. Yan, M. Han, Y. Shi, A. Badea, Y. Yang, A. Kulkarni, E. Hanson, M. E. Kandel, X. Wen and F. Zhang, *Proc. Natl. Acad. Sci. U. S. A.*, 2017, **114**, E9455–E9464.
- 5 Y. Kim, G. A. Parada, S. Liu and X. Zhao, *Sci. Rob.*, 2019, **4**, eaax7329.
- 6 Y. Kim, E. Genevriere, P. Harker, J. Choe, M. Balicki, R. W. Regenhardt, J. E. Vranic, A. A. Dmytriw, A. B. Patel and X. Zhao, *Sci. Rob.*, 2022, **7**, eabg9907.
- 7 H. Deng, K. Sattari, Y. Xie, P. Liao, Z. Yan and J. Lin, *Nat. Commun.*, 2020, **11**, 1–10.
- 8 J. Li, B. E.-F. de Ávila, W. Gao, L. Zhang and J. Wang, *Sci. Rob.*, 2017, **2**, eaam6431.
- 9 C. Laschi, B. Mazzolai and M. Cianchetti, *Sci. Rob.*, 2016, **1**, eaah3690.
- 10 W. Wang, Q. Liu, I. Tanasijevic, M. F. Reynolds, A. J. Cortese, M. Z. Miskin, M. C. Cao, D. A. Muller, A. C. Molnar and E. Lauga, *Nature*, 2022, **605**, 681–686.
- 11 C. Dillinger, N. Nama and D. Ahmed, *Nat. Commun.*, 2021, **12**, 1–11.
- 12 N. Xia, B. Jin, D. Jin, Z. Yang, C. Pan, Q. Wang, F. Ji, V. Iacovacci, C. Majidi, Y. Ding and L. Zhang, *Adv. Mater.*, 2022, **34**, 2109126.
- 13 Z. Ren, W. Hu, X. Dong and M. Sitti, *Nat. Commun.*, 2019, **10**, 1–12.
- 14 T. Wang, Z. Ren, W. Hu, M. Li and M. Sitti, *Sci. Rob.*, 2021, **7**, eabf7364.
- 15 M. Sun, C. Tian, L. Mao, X. Meng, X. Shen, B. Hao, X. Wang, H. Xie and L. Zhang, *Adv. Funct. Mater.*, 2022, **32**, 2112508.
- 16 B. Wang, K. F. Chan, K. Yuan, Q. Wang, X. Xia, L. Yang, H. Ko, Y.-X. J. Wang, J. J. Y. Sung, P. W. Y. Chiu and L. Zhang, *Sci. Rob.*, 2021, **6**, eabd2813.
- 17 M. Cianchetti, C. Laschi, A. Menciassi and P. Dario, *Nat. Rev. Mater.*, 2018, **3**, 143–153.
- 18 B. Wang, K. Kostarelos, B. J. Nelson and L. Zhang, *Adv. Mater.*, 2021, **33**, 2002047.
- 19 D. Ahmed, T. Baasch, B. Jang, S. Pane, J. Dual and B. J. Nelson, *Nano Lett.*, 2016, **16**, 4968–4974.
- 20 D. Ahmed, T. Baasch, N. Blondel, N. Läubli, J. Dual and B. J. Nelson, *Nat. Commun.*, 2017, **8**, 1–8.
- 21 T.-Y. Huang, H.-W. Huang, D. Jin, Q. Chen, J. Huang, L. Zhang and H. Duan, *Sci. Adv.*, 2020, **6**, eaav8219.
- 22 D. Jin, Q. Chen, T.-Y. Huang, J. Huang, L. Zhang and H. Duan, *Mater. Today*, 2020, **32**, 19–25.
- 23 C. Li, Y. Xue, M. Han, L. C. Palmer, J. A. Rogers, Y. Huang and S. I. Stupp, *Matter*, 2021, **4**, 1377–1390.
- 24 C. Li, A. Iscen, H. Sai, K. Sato, N. A. Sather, S. M. Chin, Z. Álvarez, L. C. Palmer, G. C. Schatz and S. I. Stupp, *Nat. Mater.*, 2020, **19**, 900–909.
- 25 R. Li, D. Jin, D. Pan, S. Ji, C. Xin, G. Liu, S. Fan, H. Wu, J. Li and Y. Hu, *ACS Nano*, 2020, **14**, 5233–5242.
- 26 W. Hu, G. Z. Lum, M. Mastrangeli and M. Sitti, *Nature*, 2018, **554**, 81–85.
- 27 Y. Kim, H. Yuk, R. Zhao, S. A. Chester and X. Zhao, *Nature*, 2018, **558**, 274–279.
- 28 T. Xu, J. Zhang, M. Salehizadeh, O. Onaizah and E. Diller, *Sci. Rob.*, 2019, **4**, eaav4494.
- 29 L. Su, D. D. Jin, C. F. Pan, N. Xia, K. F. Chan, V. Iacovacci, T. Xu, X. Du and L. Zhang, *Bioinspiration Biomimetics*, 2021, **16**, 055005.
- 30 Y. Dong, L. Wang, N. Xia, Y. Wang, S. Wang, Z. Yang, D. Jin, X. Du, E. Yu, C. Pan, B. Liu and L. Zhang, *Nano Energy*, 2021, **88**, 106254.
- 31 H. Zhou, C. C. Mayorga-Martinez, S. Pané, L. Zhang and M. Pumera, *Chem. Rev.*, 2021, **121**, 4999–5041.
- 32 Z. Ren, R. Zhang, R. H. Soon, Z. Liu, W. Hu, P. R. Onck and M. Sitti, *Sci. Adv.*, 2021, **7**, eabh2022.
- 33 B. J. Nelson, S. Gervasoni, P. W. Chiu, L. Zhang and A. Zemmar, *Proc. IEEE*, 2022, **110**, 1028–1037.
- 34 C. Tang, B. Du, S. Jiang, Q. Shao, X. Dong, X.-J. Liu and H. Zhao, *Sci. Rob.*, 2022, **7**, eabm8597.
- 35 Z. Qi, M. Zhou, Y. Li, Z. Xia, W. Huo and X. Huang, *Adv. Mater. Technol.*, 2021, **6**, 2001124.
- 36 X. Yang, W. Shang, H. Lu, Y. Liu, L. Yang, R. Tan, X. Wu and Y. Shen, *Sci. Rob.*, 2020, **5**, eabc8191.
- 37 Y. Dong, L. Wang, N. Xia, Z. Yang, C. Zhang, C. Pan, D. Jin, J. Zhang, C. Majidi and L. Zhang, *Sci. Adv.*, 2022, **8**, eabn8932.
- 38 Y. Harduf, D. Jin, Y. Or and L. Zhang, *Soft Rob.*, 2018, **5**, 389–398.
- 39 M. Z. Miskin, A. J. Cortese, K. Dorsey, E. P. Esposito, M. F. Reynolds, Q. Liu, M. Cao, D. A. Muller, P. L. McEuen and I. Cohen, *Nature*, 2020, **584**, 557–561.
- 40 X. Kuang, S. Wu, Q. Ze, L. Yue, Y. Jin, S. M. Montgomery, F. Yang, H. J. Qi and R. Zhao, *Adv. Mater.*, 2021, **33**, 2102113.

41 Z. Fang, H. Song, Y. Zhang, B. Jin, J. Wu, Q. Zhao and T. Xie, *Matter*, 2020, **2**, 1187–1197.

42 Y. Zhang, Z. Wang, Y. Yang, Q. Chen, X. Qian, Y. Wu, H. Liang, Y. Xu, Y. Wei and Y. Ji, *Sci. Adv.*, 2020, **6**, eaay8606.

43 S. Zhang, X. Ke, Q. Jiang, H. Ding and Z. Wu, *Sci. Rob.*, 2021, **6**, eabd6107.

44 Y. Zhao, C.-Y. Lo, L. Ruan, C.-H. Pi, C. Kim, Y. Alsaid, I. Frenkel, R. Rico, T.-C. Tsao and X. He, *Sci. Rob.*, 2021, **6**, eabd5483.

45 M. A. Skylar-Scott, J. Mueller, C. W. Visser and J. A. Lewis, *Nature*, 2019, **575**, 330–335.

46 D. Rus and M. T. Tolley, *Nat. Rev. Mater.*, 2018, **3**, 101–112.

47 S. Palagi and P. Fischer, *Nat. Rev. Mater.*, 2018, **3**, 113–124.

48 L. Hines, K. Petersen, G. Z. Lum and M. Sitti, *Adv. Mater.*, 2017, **29**, 1603483.

49 J. Yu, D. Jin, K.-F. Chan, Q. Wang, K. Yuan and L. Zhang, *Nat. Commun.*, 2019, **10**, 1–12.

50 J. Yu, B. Wang, X. Du, Q. Wang and L. Zhang, *Nat. Commun.*, 2018, **9**, 1–9.

51 Y. Kim and X. Zhao, *Chem. Rev.*, 2022, **122**, 5317–5364.

52 T. Qiu, T.-C. Lee, A. G. Mark, K. I. Morozov, R. Münster, O. Mierka, S. Turek, A. M. Leshansky and P. Fischer, *Nat. Commun.*, 2014, **5**, 1–8.

53 H. Lu, M. Zhang, Y. Yang, Q. Huang, T. Fukuda, Z. Wang and Y. Shen, *Nat. Commun.*, 2018, **9**, 1–7.

54 H. Song, H. Lee, J. Lee, J. K. Choe, S. Lee, J. Y. Yi, S. Park, J.-W. Yoo, M. S. Kwon and J. Kim, *Nano Lett.*, 2020, **20**, 5185–5192.

55 J. Cui, T.-Y. Huang, Z. Luo, P. Testa, H. Gu, X.-Z. Chen, B. J. Nelson and L. J. Heyderman, *Nature*, 2019, **575**, 164–168.

56 Y. Alapan, A. C. Karacakol, S. N. Guzelhan, I. Isik and M. Sitti, *Sci. Adv.*, 2020, **6**, eabc6414.

57 J. Zhang, Z. Ren, W. Hu, R. H. Soon, I. C. Yasa, Z. Liu and M. Sitti, *Sci. Rob.*, 2021, **6**, eabf0112.

58 Z. Liu, M. Li, X. Dong, Z. Ren, W. Hu and M. Sitti, *Nat. Commun.*, 2022, **13**, 1–11.

59 S. Li, M. M. Lerch, J. T. Waters, B. Deng, R. S. Martens, Y. Yao, D. Y. Kim, K. Bertoldi, A. Grinthal and A. C. Balazs, *Nature*, 2022, **605**, 76–83.

60 M. Lahikainen, H. Zeng and A. Priimagi, *Nat. Commun.*, 2018, **9**, 1–8.

61 L. Ren, N. Nama, J. M. McNeill, F. Soto, Z. Yan, W. Liu, W. Wang, J. Wang and T. E. Mallouk, *Sci. Adv.*, 2019, **5**, eaax3084.

62 A. Aghakhani, A. Pena-Francesch, U. Bozuyuk, H. Cetin, P. Wrede and M. Sitti, *Sci. Adv.*, 2022, **8**, eabm5126.

63 K. Melde, A. G. Mark, T. Qiu and P. Fischer, *Nature*, 2016, **537**, 518–522.

64 S. Yang, Z. Tian, Z. Wang, J. Rufo, P. Li, J. Mai, J. Xia, H. Bachman, P.-H. Huang and M. Wu, *Nat. Mater.*, 2022, **21**, 540–546.

65 C. Y. Li, S. Y. Zheng, X. P. Hao, W. Hong, Q. Zheng and Z. L. Wu, *Sci. Adv.*, 2022, **8**, eabm9608.

66 J. Pu, Y. Meng, Z. Xie, Z. Peng, J. Wu, Y. Shi, R. Plamthottam, W. Yang and Q. Pei, *Sci. Adv.*, 2022, **8**, eabm6200.

67 D. Han, C. Farino, C. Yang, T. Scott, D. Browe, W. Choi, J. W. Freeman and H. Lee, *ACS Appl. Mater. Interfaces*, 2018, **10**, 17512–17518.

68 Q. Ze, X. Kuang, S. Wu, J. Wong, S. M. Montgomery, R. Zhang, J. M. Kovitz, F. Yang, H. J. Qi and R. Zhao, *Adv. Mater.*, 2020, **32**, 1906657.

69 J. Zhang, Y. Guo, W. Hu, R. H. Soon, Z. S. Davidson and M. Sitti, *Adv. Mater.*, 2021, **33**, 2006191.

70 X.-Q. Wang, C. F. Tan, K. H. Chan, X. Lu, L. Zhu, S.-W. Kim and G. W. Ho, *Nat. Commun.*, 2018, **9**, 1–10.

71 X. Z. Chen, B. Jang, D. Ahmed, C. Hu, C. De Marco, M. Hoop, F. Mushtaq, B. J. Nelson and S. Pané, *Adv. Mater.*, 2018, **30**, 1705061.

72 V. K. Bandari, Y. Nan, D. Karnaushenko, Y. Hong, B. Sun, F. Striggow, D. D. Karnaushenko, C. Becker, M. Faghah and M. Medina-Sánchez, *Nat. Electron.*, 2020, **3**, 172–180.

73 S. Maeda, Y. Hara, T. Sakai, R. Yoshida and S. Hashimoto, *Adv. Mater.*, 2007, **19**, 3480–3484.

74 E. Siéfert, E. Reyssat, J. Bico and B. Roman, *Nat. Mater.*, 2019, **18**, 24–28.

75 C. Tawk and G. Aliche, *Adv. Intell. Syst.*, 2021, **3**, 2000223.

76 L. Sun, Y. Yu, Z. Chen, F. Bian, F. Ye, L. Sun and Y. Zhao, *Chem. Soc. Rev.*, 2020, **49**, 4043–4069.

77 F. Striggow, M. Medina-Sánchez, G. K. Auernhammer, V. Magdanz, B. M. Friedrich and O. G. Schmidt, *Small*, 2020, **16**, 2000213.

78 F. Fu, L. Shang, Z. Chen, Y. Yu and Y. Zhao, *Sci. Rob.*, 2018, **3**, eaar8580.

79 V. Magdanz, I. S. Khalil, J. Simmchen, G. P. Furtado, S. Mohanty, J. Gebauer, H. Xu, A. Klingner, A. Aziz and M. Medina-Sánchez, *Sci. Adv.*, 2020, **6**, eaba5855.

80 R. K. Katzschatmann, J. DelPreto, R. MacCurdy and D. Rus, *Sci. Rob.*, 2018, **3**, eaar3449.

81 D. R. Yoerger, A. F. Govindarajan, J. C. Howland, J. K. Llopiz, P. H. Wiebe, M. Curran, J. Fujii, D. Gomez-Ibanez, K. Katija and B. H. Robison, *Sci. Rob.*, 2021, **6**, eabe1901.

82 J. Lee, Y. Yoon, H. Park, J. Choi, Y. Jung, S. H. Ko and W.-H. Yeo, *Adv. Intell. Syst.*, 2022, 2100271.

83 P. Won, S. H. Ko, C. Majidi, A. W. Feinberg and V. A. Webster-Wood, *Actuators*, 2020, **9**, 96.

84 V. Magdanz, S. Sanchez and O. G. Schmidt, *Adv. Mater.*, 2013, **25**, 6581–6588.

85 J. A.-C. Liu, J. H. Gillen, S. R. Mishra, B. A. Evans and J. B. Tracy, *Sci. Adv.*, 2019, **5**, eaaw2897.

86 B. Han, Z. C. Ma, Y. L. Zhang, L. Zhu, H. Fan, B. Bai, Q. D. Chen, G. Z. Yang and H. B. Sun, *Adv. Funct. Mater.*, 2022, **32**, 2110997.

87 J. Li, X. Li, T. Luo, R. Wang, C. Liu, S. Chen, D. Li, J. Yue, S.-h Cheng and D. Sun, *Sci. Rob.*, 2018, **3**, eaat8829.

88 H. Lee, Y. Jang, J. K. Choe, S. Lee, H. Song, J. P. Lee, N. Lone and J. Kim, *Sci. Rob.*, 2020, **5**, eaay9024.

89 Z. Zhu, D. W. H. Ng, H. S. Park and M. C. McAlpine, *Nat. Rev. Mater.*, 2021, **6**, 27–47.

90 S.-J. Jeon, A. W. Hauser and R. C. Hayward, *Acc. Chem. Res.*, 2017, **50**, 161–169.

91 D. Jin and L. Zhang, *Acc. Chem. Res.*, 2021, **55**, 98–109.

92 S. Wei, W. Lu, X. Le, C. Ma, H. Lin, B. Wu, J. Zhang, P. Theato and T. Chen, *Angew. Chem.*, 2019, **131**, 16389–16397.

93 M. Li, A. Pal, A. Aghakhani, A. Pena-Francesch and M. Sitti, *Nat. Rev. Mater.*, 2022, **7**, 235–249.

94 S. Sundaram, M. Skouras, D. S. Kim, L. van den Heuvel and W. Matusik, *Sci. Adv.*, 2019, **5**, eaaw1160.

95 S. Jeon, S. Kim, S. Ha, S. Lee, E. Kim, S. Y. Kim, S. H. Park, J. H. Jeon, S. W. Kim and C. Moon, *Sci. Rob.*, 2019, **4**, eaav4317.

96 G. Go, S.-G. Jeong, A. Yoo, J. Han, B. Kang, S. Kim, K. T. Nguyen, Z. Jin, C.-S. Kim and Y. R. Seo, *Sci. Rob.*, 2020, **5**, eaay6626.

97 I. Van Meerbeek, C. De Sa and R. Shepherd, *Sci. Rob.*, 2018, **3**, eaau2489.

98 X. Wang, R. Guo and J. Liu, *Adv. Mater. Technol.*, 2019, **4**, 1800549.

99 Y. Ohm, C. Pan, M. J. Ford, X. Huang, J. Liao and C. Majidi, *Nat. Electron.*, 2021, **4**, 185–192.

100 M. Han, L. Chen, K. Aras, C. Liang, X. Chen, H. Zhao, K. Li, N. R. Faye, B. Sun and J.-H. Kim, *Nat. Biomed. Eng.*, 2020, **4**, 997–1009.

101 H. Song, G. Luo, Z. Ji, R. Bo, Z. Xue, D. Yan, F. Zhang, K. Bai, J. Liu and X. Cheng, *Sci. Adv.*, 2022, **8**, eabm3785.

102 H. Lu, Y. Hong, Y. Yang, Z. Yang and Y. Shen, *Adv. Sci.*, 2020, **7**, 2000069.

103 L. Peng, Y. Zhang, J. Wang, Q. Wang, G. Zheng, Y. Li, Z. Chen, Y. Chen, L. Jiang and C.-P. Wong, *Nano Energy*, 2022, 107367.

104 Y. Wang, H. Cui, Q. Zhao and X. Du, *Matter*, 2019, **1**, 626–638.

105 S. Xu, Z. Yan, K.-I. Jang, W. Huang, H. Fu, J. Kim, Z. Wei, M. Flavin, J. McCracken and R. Wang, *Science*, 2015, **347**, 154–159.

106 Y. Zhang, F. Zhang, Z. Yan, Q. Ma, X. Li, Y. Huang and J. A. Rogers, *Nat. Rev. Mater.*, 2017, **2**, 1–17.

107 F. Gabler, D. D. Karnaushenko, D. Karnaushenko and O. G. Schmidt, *Nat. Commun.*, 2019, **10**, 1–10.

108 L. Miao, Y. Song, Z. Ren, C. Xu, J. Wan, H. Wang, H. Guo, Z. Xiang, M. Han and H. Zhang, *Adv. Mater.*, 2021, **33**, 2102691.

109 B. Rivkin, C. Becker, B. Singh, A. Aziz, F. Akbar, A. Egunov, D. D. Karnaushenko, R. Naumann, R. Schäfer and M. Medina-Sánchez, *Sci. Adv.*, 2021, **7**, eabl5408.

110 C. Xu and W. Gao, *Nat. Electron.*, 2020, **3**, 139–140.

111 S. Terryn, J. Langenbach, E. Roels, J. Brancart, C. Bakkali-Hassani, Q.-A. Poutrel, A. Georgopoulou, T. G. Thuruthel, A. Safaei and P. Ferrentino, *Mater. Today*, 2021, **47**, 187–205.

112 E. J. Markvicka, M. D. Bartlett, X. Huang and C. Majidi, *Nat. Mater.*, 2018, **17**, 618–624.

113 C. H. Li and J. L. Zuo, *Adv. Mater.*, 2020, **32**, 1903762.

114 S. Terryn, J. Brancart, D. Lefever, G. Van Assche and B. Vanderborght, *Sci. Rob.*, 2017, **2**, eaan4268.

115 H. Qin, T. Zhang, N. Li, H.-P. Cong and S.-H. Yu, *Nat. Commun.*, 2019, **10**, 1–11.

116 J. Cao, C. Zhou, G. Su, X. Zhang, T. Zhou, Z. Zhou and Y. Yang, *Adv. Mater.*, 2019, **31**, 1900042.

117 M. Caprioli, I. Roppolo, A. Chiappone, L. Larush, C. F. Pirri and S. Magdassi, *Nat. Commun.*, 2021, **12**, 1–9.

118 Q. Zhou, F. Gardea, Z. Sang, S. Lee, M. Pharr and S. A. Sukhishvili, *Adv. Funct. Mater.*, 2020, **30**, 2002374.

119 Y. Zhang, X.-Y. Yin, M. Zheng, C. Moorlag, J. Yang and Z. L. Wang, *J. Mater. Chem. A*, 2019, **7**, 6972–6984.

120 X. Li, R. Yu, Y. He, Y. Zhang, X. Yang, X. Zhao and W. Huang, *ACS Macro Lett.*, 2019, **8**, 1511–1516.

121 K. Yu, A. Xin, H. Du, Y. Li and Q. Wang, *NPG Asia Mater.*, 2019, **11**, 1–11.

122 Y. Cheng, K. H. Chan, X. Q. Wang, T. Ding, T. Li, C. Zhang, W. Lu, Y. Zhou and G. W. Ho, *Adv. Funct. Mater.*, 2021, **31**, 2101825.

123 Y. Wu, S. Zhang, Y. Yang, Z. Li, Y. Wei and Y. Ji, *Sci. Adv.*, 2022, **8**, eab06021.

124 S. M. Montgomery, S. Wu, X. Kuang, C. D. Armstrong, C. Zemelka, Q. Ze, R. Zhang, R. Zhao and H. J. Qi, *Adv. Funct. Mater.*, 2021, **31**, 2005319.

125 S. Wu, Q. Ze, R. Zhang, N. Hu, Y. Cheng, F. Yang and R. Zhao, *ACS Appl. Mater. Interfaces*, 2019, **11**, 41649–41658.

126 J. Zhang, Y. Guo, W. Hu and M. Sitti, *Adv. Mater.*, 2021, **33**, 2100336.

127 Y. Wu, X. Dong, J.-k Kim, C. Wang and M. Sitti, *Sci. Adv.*, 2022, **8**, eabn3431.

128 J. Liu, Y. Yao, X. Li and Z. Zhang, *Chem. Eng. J.*, 2021, **408**, 127262.

129 S. Liang, X. Qiu, J. Yuan, W. Huang, X. Du and L. Zhang, *ACS Appl. Mater. Interfaces*, 2018, **10**, 19123–19132.

130 A. Rafsanjani, Y. Zhang, B. Liu, S. M. Rubinstein and K. Bertoldi, *Sci. Rob.*, 2018, **3**, eaar7555.

131 J. W. Booth, D. Shah, J. C. Case, E. L. White, M. C. Yuen, O. Cyr-Choiniere and R. Kramer-Bottiglio, *Sci. Rob.*, 2018, **3**, eaat1853.

132 Y. Wang, X. Yang, Y. Chen, D. K. Wainwright, C. P. Kenaley, Z. Gong, Z. Liu, H. Liu, J. Guan and T. Wang, *Sci. Rob.*, 2017, **2**, eaan8072.

133 X. Ke, S. Zhang, Z. Chai, J. Jiang, Y. Xu, B. Tao, H. Ding and Z. Wu, *Mater. Today Phys.*, 2021, **17**, 100313.

134 Y. Liu, B. Shaw, M. D. Dickey and J. Genzer, *Sci. Adv.*, 2017, **3**, e1602417.

135 P. Cabanach, A. Pena-Francesch, D. Sheehan, U. Bozuyuk, O. Yasa, S. Borros and M. Sitti, *Adv. Mater.*, 2020, **32**, 2003013.

136 C. Kaspar, B. Ravoo, W. G. van der Wiel, S. Wegner and W. Pernice, *Nature*, 2021, **594**, 345–355.

137 M. Sitti, *Extreme Mech. Lett.*, 2021, **46**, 101340.

138 J. Kim, S. E. Choi, H. Lee and S. Kwon, *Adv. Mater.*, 2013, **25**, 1415–1419.

139 H. Zeng, H. Zhang, O. Ikkala and A. Priimagi, *Matter*, 2020, **2**, 194–206.

140 M. Gao, Y. Meng, C. Shen and Q. Pei, *Adv. Mater.*, 2022, 2109798.

141 Y. Wei, Y. Chen, T. Ren, Q. Chen, C. Yan, Y. Yang and Y. Li, *Soft Rob.*, 2016, **3**, 134–143.

142 S. Jadhav, M. R. A. Majit, B. Shih, J. P. Schulze and M. T. Tolley, *Soft Rob.*, 2022, **9**, 173–186.

143 I. Ha, M. Kim, K. K. Kim, S. Hong, H. Cho, J. Kwon, S. Han, Y. Yoon, P. Won and S. H. Ko, *Adv. Sci.*, 2021, **8**, 2102536.

144 H. Ceylan, N. O. Dogan, I. C. Yasa, M. N. Musaoglu, Z. U. Kulali and M. Sitti, *Sci. Adv.*, 2021, **7**, eabhw0273.

145 W. Zhu, J. Li, Y. J. Leong, I. Rozen, X. Qu, R. Dong, Z. Wu, W. Gao, P. H. Chung and J. Wang, *Adv. Mater.*, 2015, **27**, 4411–4417.

146 T. Y. Huang, M. S. Sakar, A. Mao, A. J. Petruska, F. Qiu, X. B. Chen, S. Kennedy, D. Mooney and B. J. Nelson, *Adv. Mater.*, 2015, **27**, 6644–6650.

147 X. Wang, X. H. Qin, C. Hu, A. Terzopoulou, X. Z. Chen, T. Y. Huang, K. Maniura-Weber, S. Pané and B. J. Nelson, *Adv. Funct. Mater.*, 2018, **28**, 1804107.

148 Y. Yang, X. Li, M. Chu, H. Sun, J. Jin, K. Yu, Q. Wang, Q. Zhou and Y. Chen, *Sci. Adv.*, 2019, **5**, eaau9490.

149 R. L. Truby and J. A. Lewis, *Nature*, 2016, **540**, 371–378.

150 Y. Cheng, K. H. Chan, X.-Q. Wang, T. Ding, T. Li, X. Lu and G. W. Ho, *ACS Nano*, 2019, **13**, 13176–13184.

151 A. K. Mishra, T. J. Wallin, W. Pan, P. Xu, K. Wang, E. P. Giannelis, B. Mazzolai and R. F. Shepherd, *Sci. Rob.*, 2020, **5**, eaaz3918.

152 L. Y. Zhou, J. Fu and Y. He, *Adv. Funct. Mater.*, 2020, **30**, 2000187.

153 N. Xia, D. Jin, V. Iacovacci and L. Zhang, *Multifunct. Mater.*, 2022, **5**, 012001.

154 Q. Ge, Z. Chen, J. Cheng, B. Zhang, Y.-F. Zhang, H. Li, X. He, C. Yuan, J. Liu and S. Magdassi, *Sci. Adv.*, 2021, **7**, eaba4261.

155 Z.-C. Ma, Y.-L. Zhang, B. Han, X.-Y. Hu, C.-H. Li, Q.-D. Chen and H.-B. Sun, *Nat. Commun.*, 2020, **11**, 1–10.

156 R. L. Truby, M. Wehner, A. K. Grosskopf, D. M. Vogt, S. G. Uzel, R. J. Wood and J. A. Lewis, *Adv. Mater.*, 2018, **30**, 1706383.

157 H. Cui, D. Yao, R. Hensleigh, H. Lu, A. Calderon, Z. Xu, S. Davaria, Z. Wang, P. Mercier and P. Tarazaga, *Science*, 2022, **376**, 1287–1293.

158 A. Sydney Gladman, E. A. Matsumoto, R. G. Nuzzo, L. Mahadevan and J. A. Lewis, *Nat. Mater.*, 2016, **15**, 413–418.

159 X. Kuang, D. J. Roach, J. Wu, C. M. Hamel, Z. Ding, T. Wang, M. L. Dunn and H. J. Qi, *Adv. Funct. Mater.*, 2019, **29**, 1805290.

160 Y. Piskarev, J. Shintake, C. Chautems, J. Lussi, Q. Boehler, B. J. Nelson and D. Floreano, *Adv. Funct. Mater.*, 2022, 2107662.

161 M. Mattmann, C. De Marco, F. Briatico, S. Tagliabue, A. Colusso, X. Z. Chen, J. Lussi, C. Chautems, S. Pané and B. Nelson, *Adv. Sci.*, 2022, **9**, 2103277.

162 J. Lussi, M. Mattmann, S. Sevim, F. Grigis, C. De Marco, C. Chautems, S. Pané, J. Puigmarti-Luis, Q. Boehler and B. J. Nelson, *Adv. Sci.*, 2021, **8**, 2101290.

163 T. Zhang, L. Yang, X. Yang, R. Tan, H. Lu and Y. Shen, *Adv. Intell. Syst.*, 2021, **3**, 2000189.

164 T. Gopesh, J. H. Wen, D. Santiago-Dieppa, B. Yan, J. S. Pannell, A. Khalessi, A. Norbash and J. Friend, *Sci. Rob.*, 2021, **6**, eabf0601.

165 Z. Yang, L. Yang, M. Zhang, Q. Wang, S. C. H. Yu and L. Zhang, *IEEE Rob. Autom. Lett.*, 2021, **6**, 1280–1287.

166 Z. Yang, L. Yang, M. Zhang, C. Zhang, S. C. H. Yu and L. Zhang, *IEEE/ASME Trans. Mechatron.*, 2021, DOI: [10.1109/TMECH.2021.3121267](https://doi.org/10.1109/TMECH.2021.3121267).

167 M. McCandless, A. Perry, N. DiFilippo, A. Carroll, E. Billatos and S. Russo, *Soft Rob.*, 2022, **9**, 754–766.

168 Z. Yang, L. Yang, M. Zhang, N. Xia and L. Zhang, *IEEE Trans. Ind. Electron.*, 2022, **70**, 614–623.

169 L. Wang, D. Zheng, P. Harker, A. B. Patel, C. F. Guo and X. Zhao, *Proc. Natl. Acad. Sci. U. S. A.*, 2021, **118**, e2021922118.

170 C. Chautems, A. Tonazzini, Q. Boehler, S. H. Jeong, D. Floreano and B. J. Nelson, *Adv. Intell. Syst.*, 2020, **2**, 1900086.

171 Q. Wang, K. F. Chan, K. Schweizer, X. Du, D. Jin, S. C. H. Yu, B. J. Nelson and L. Zhang, *Sci. Adv.*, 2021, **7**, eabe5914.

172 X. Yan, Q. Zhou, M. Vincent, Y. Deng, J. Yu, J. Xu, T. Xu, T. Tang, L. Bian and Y.-X. J. Wang, *Sci. Rob.*, 2017, **2**, eaqq1155.

173 M. Sitti, *Nat. Rev. Mater.*, 2018, **3**, 74–75.

174 X. Yan, Q. Zhou, J. Yu, T. Xu, Y. Deng, T. Tang, Q. Feng, L. Bian, Y. Zhang and A. Ferreira, *Adv. Funct. Mater.*, 2015, **25**, 5333–5342.

175 J. Park, J. y Kim, S. Pane, B. J. Nelson and H. Choi, *Adv. Healthcare Mater.*, 2021, **10**, 2001096.

176 M. Dong, X. Wang, X. Z. Chen, F. Mushtaq, S. Deng, C. Zhu, H. Torlakcik, A. Terzopoulou, X. H. Qin and X. Xiao, *Adv. Funct. Mater.*, 2020, **30**, 1910323.

177 X. Liu, J. Liu, S. Lin and X. Zhao, *Mater. Today*, 2020, **36**, 102–124.

178 X. Du, H. Cui, T. Xu, C. Huang, Y. Wang, Q. Zhao, Y. Xu and X. Wu, *Adv. Funct. Mater.*, 2020, **30**, 1909202.

179 C. Wang, K. Sim, J. Chen, H. Kim, Z. Rao, Y. Li, W. Chen, J. Song, R. Verduzco and C. Yu, *Adv. Mater.*, 2018, **30**, 1706695.

180 H. Wang, M. Totaro and L. Beccai, *Adv. Sci.*, 2018, **5**, 1800541.

181 Y. Pang, X. Xu, S. Chen, Y. Fang, X. Shi, Y. Deng, Z.-L. Wang and C. Cao, *Nano Energy*, 2022, 107137.

182 Y. C. Lai, J. Deng, R. Liu, Y. C. Hsiao, S. L. Zhang, W. Peng, H. M. Wu, X. Wang and Z. L. Wang, *Adv. Mater.*, 2018, **30**, 1801114.

183 H. Kim, H. Lee, I. Ha, J. Jung, P. Won, H. Cho, J. Yeo, S. Hong, S. Han and J. Kwon, *Adv. Funct. Mater.*, 2018, **28**, 1801847.

184 H. Kim, J. Choi, K. K. Kim, P. Won, S. Hong and S. H. Ko, *Nat. Commun.*, 2021, **12**, 1–11.

185 J. Lee, H. Sul, Y. Jung, H. Kim, S. Han, J. Choi, J. Shin, D. Kim, J. Jung and S. Hong, *Adv. Funct. Mater.*, 2020, **30**, 2003328.

186 P. Won, K. K. Kim, H. Kim, J. J. Park, I. Ha, J. Shin, J. Jung, H. Cho, J. Kwon and H. Lee, *Adv. Mater.*, 2021, **33**, 2002397.

187 C. Christianson, C. Bayag, G. Li, S. Jadhav, A. Giri, C. Agba, T. Li and M. T. Tolley, *Front. Rob. AI*, 2019, **6**, 126.

188 P. Li, Y. Wang, U. Gupta, J. Liu, L. Zhang, D. Du, C. C. Foo, J. Ouyang and J. Zhu, *Adv. Funct. Mater.*, 2019, **29**, 1901908.

189 H. Lee, H. Kim, I. Ha, J. Jung, P. Won, H. Cho, J. Yeo, S. Hong, S. Han and J. Kwon, *Soft Rob.*, 2019, **6**, 760–767.

190 L. S. Novelino, Q. Ze, S. Wu, G. H. Paulino and R. Zhao, *Proc. Natl. Acad. Sci. U. S. A.*, 2020, **117**, 24096–24101.

191 K. Bai, X. Cheng, Z. Xue, H. Song, L. Sang, F. Zhang, F. Liu, X. Luo, W. Huang and Y. Huang, *Sci. Adv.*, 2020, **6**, eabb7417.

192 H. Kim, S.-k Ahn, D. M. Mackie, J. Kwon, S. H. Kim, C. Choi, Y. H. Moon, H. B. Lee and S. H. Ko, *Mater. Today*, 2020, **41**, 243–269.

193 X. Cheng and Y. Zhang, *Adv. Mater.*, 2019, **31**, 1901895.

194 J. K. Park, K. Nan, H. Luan, N. Zheng, S. Zhao, H. Zhang, X. Cheng, H. Wang, K. Li and T. Xie, *Adv. Mater.*, 2019, **31**, 1905715.

195 L. Rivera-Tarazona, V. Bhat, H. Kim, Z. Campbell and T. Ware, *Sci. Adv.*, 2020, **6**, eaax8582.

196 G. Cai, J.-H. Ciou, Y. Liu, Y. Jiang and P. S. Lee, *Sci. Adv.*, 2019, **5**, eaaw7956.

197 S. Li, R. Batra, D. Brown, H.-D. Chang, N. Ranganathan, C. Hoberman, D. Rus and H. Lipson, *Nature*, 2019, **567**, 361–365.

198 W. Wang, J. Giltinan, S. Zakharchenko and M. Sitti, *Sci. Adv.*, 2017, **3**, e1602522.

199 Y. Alapan, B. Yigit, O. Beker, A. F. Demirörs and M. Sitti, *Nat. Mater.*, 2019, **18**, 1244–1251.

200 G. Gardi, S. Ceron, W. Wang, K. Petersen and M. Sitti, *Nat. Commun.*, 2022, **13**, 1–14.

201 L. Yang, J. Jiang, X. Gao, Q. Wang, Q. Dou and L. Zhang, *Nat. Mach. Intell.*, 2022, **4**, 480–493.

202 S. O. Demir, U. Culha, A. C. Karacakol, A. Pena-Francesch, S. Trimpe and M. Sitti, *Int. J. Rob. Res.*, 2021, **40**, 1331–1351.